Acta Astronautica 94 (2014) 116–131

Contents lists available at ScienceDirect

Acta Astronautica

journal homepage: www.elsevier.com/locate/actaastro

Stability and shape analysis of relative equilibrium for three-spacecraft electromagnetic formation

Huan Huang, Yan-wei Zhu*, Le-ping Yang, Yuan-wen Zhang

College of Aerospace Science and Engineering, National University of Defense Technology, Changsha, 410073 Hunan, PR China

ARTICLE INFO

Article history:
Received 1 February 2013
Received in revised form
11 August 2013
Accepted 17 August 2013
Available online 26 August 2013

Keywords:
Electromagnetic formation
Relative equilibrium
Collinear/triangular configuration
Invariant shape
Stability

ABSTRACT

The invariant shapes for close formation flying with inter-craft electromagnetic force ensure several potential space applications. However, the 6-DOF relative equilibrium problem has not been systematically investigated. This paper mainly analyzes the invariant shapes of relative equilibrium for the three-spacecraft electromagnetic formation, and studies the families of invariant shape solutions with real and constant magnetic moments as well as their linear stability. The problem is examined based on the full nonlinear coupled dynamic models for collinear and general triangular configurations. The relative equilibrium conditions are analyzed to determine whether an invariant shape do exist, and the corresponding families of invariant shape solutions are identified for static and spinning configurations respectively. Finally, the linear stability of such invariant shapes is numerically discussed, which have shown that most invariant shapes are unstable and controllable.

1. Introduction

Close formation flying of spacecraft with separation distances on the order of tens of meters presents several potential space applications, such as high resolution space-based imaging, spacecraft cluster, as well as wide-field-of-view optical interferometry. NASA has proposed the application of this type of formation to Terrestrial Planet Finder [1]. Propellant consumption and plume contamination coming with conventional chemical propulsion are the particular challenges for close formation flying. An attractive operational approach is applying the non-contacting inter-craft forces such as Coulomb forces or electromagnetic forces to effectively offset above shortages and offer continuous reversible and synchronous controllability to improve the precision of formation control. Coulomb formation [2] is by actively controlling the charges on various spacecrafts to control the relative positions, but the shielding effect caused by the space plasma restricts its application only in GEO or higher altitudes. Electromagnetic formation flight (EMFF) [3, 4] is proposed by using the magnetic fields electrically generated by superconducting magnetic coils equipped on all crafts, and generating coupled electromagnetic force and torque to control the relative trajectory and attitude. As an emerging approach of propellantless formation flying, EMFF allows better control authority and broader space applications.

One of the particular interests in close formation flying actuated by internal forces is invariant shapes with constant actuation, which satisfy the requirements of relative equilibrium. Here the formation maintains a fixed geometry and behaves as a single rigid body in orbit, making it convenient for formation keeping and control. Such formations are either static with respect to the orbital frame or spinning around the collective center of mass, both of which are interested

* Corresponding author. Tel.: +86 13875 859740.
E-mail address: zywnudt@163.com (Y.-w. Zhu).

0094-5765/$ - see front matter © 2013 IAA. Published by Elsevier Ltd. All rights reserved.
http://dx.doi.org/10.1016/j.actaastro.2013.08.011

in whether or not a possible shape exists with real and constant actuation, and how the internal force influences the feasibility and stability of invariant shapes. These problems serve as the inspiration for the current work.

In recent years, a significant amount of investigation on the relative equilibrium with Coulomb force has been done. Schaub [5] proposed necessary conditions for a charged static formation to exist. Berryman [6] determined the analytic charge solutions for two- and three-craft static Coulomb formation. Natarajan [7] investigated the relative equilibrium stability of two-craft Coulomb formation along orbit radial, along-track and normal direction, respectively. Inampudi [8] analyzed the linearized orbit radial dynamics and stability of a charged two-craft formation at the libration points. For the spinning case, Schaub [9] showed that the spinning two-craft Coulomb configuration is passively stable. Hussein [10] laid the groundwork for determining invariant shape solutions for the spinning three-craft Coulomb formation first, and illustrated a few particular invariant shapes with constant charges. Further, Hussein [11] derived the general conditions for the spinning charged three-craft equilibrium and examined equal mass collinear solutions to be unstable. Wang [12] developed a Lyapunov based nonlinear control strategy for a charged three-craft equilibrium collinear configuration. Hogan [13,14] proved that for any desired invariant three-craft collinear shape an infinite set of real charge solutions always exists, and described the discovery of families of multiple invariant shape solutions with set charges, as well as the linear stability analysis.

In contrast to Coulomb formation, formation flying with inter-craft electromagnetic force is not limited by the orbital altitude, and more importantly, the relative equilibrium is a 6-DOF problem since the relative attitude motion caused by coupled electromagnetic torques should be considered as well. In the field of EMFF, MIT [15–18] has systematically studied the problems of dynamics, control and ground experiment, but the research on relative equilibrium remains less. Miller [19] and Kong [20] analyzed the feasibility of electromagnetic force on spinning five-craft arrays maintenance as needed for TPF. Hussein [21] described the conditions of relative equilibrium for a planar three-craft magnetic formation, and identified three particular spinning configurations to be unstable. However, previous work is merely on symmetric cases to offer a few particular solutions, and gravity is always ignored for simplicity. In this sense, the electromagnetic equilibrium formation has not yet been systematically studied.

With above considerations in mind, this paper mainly analyzes the invariant shapes of relative equilibrium for three-craft electromagnetic formation, and describes the families of invariant shape solutions with real and constant magnetic moments, as well as the linear stability analysis on such formations. The remainder is organized as follows. Firstly, the 6-DOF nonlinear coupled dynamic models for collinear and triangular configurations are derived based on the Kane method. Secondly, the relative equilibrium for static and spinning three-craft electromagnetic formation is analyzed, and the invariant shape solutions of varied configurations are identified. Thirdly, the linear stability for different families of shape solutions is numerically discussed. Finally, some conclusions are safely put forward.

2. Problem formulation

The scope of this paper is limited to a three-craft electromagnetic formation operating in a circular orbit, and formation control is enabled solely by the electromagnetic forces and torques among spacecrafts. As depicted in Fig. 1, the position vectors from formation center of mass O_{CM} to each of the three crafts are defined as $\boldsymbol{\rho}_1$, $\boldsymbol{\rho}_2$, $\boldsymbol{\rho}_3$ respectively, and ϕ is the angle between $\boldsymbol{\rho}_1$ and $\boldsymbol{\rho}_2$. Each craft is treated as a uniform spherical rigid-body with mass m_i, and three superconducting magnetic coils are equipped orthogonally to generate a steerable magnetic moment $\boldsymbol{\mu}_i$, where $i=1, 2, 3$.

For analysis convenience, three kinds of reference frames are introduced as follows. Orbital frame $O_{CM}-\hat{x}_{CM}\hat{y}_{CM}\hat{z}_{CM}$ is noted as $\mathscr{H}$ with its origin at O_{CM}, the $\hat{x}_{CM},\hat{y}_{CM},\hat{z}_{CM}$ axes align with orbit radial, along-track and normal direction

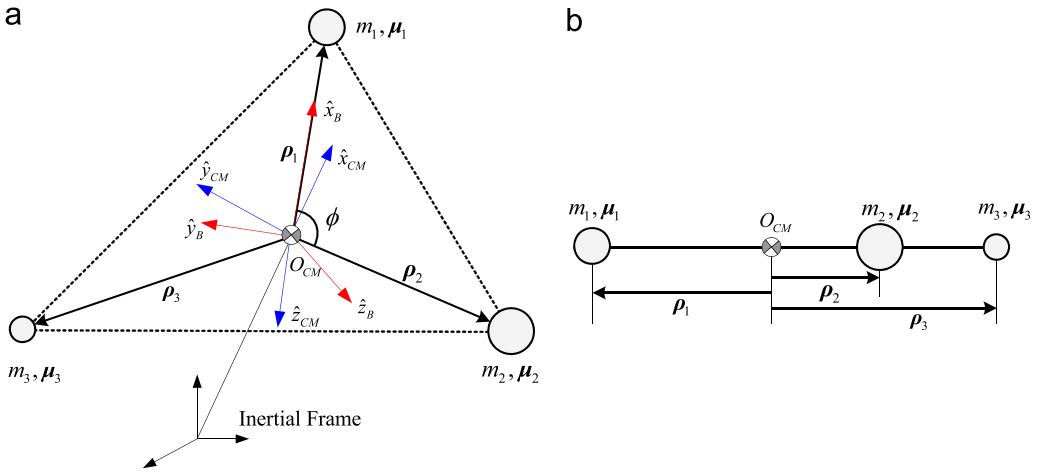

Fig. 1. Three-spacecraft electromagnetic formation. a) General triangular three-craft configuration and b) Collinear three-craft configuration.

respectively. Formation fixed frame $O_{CM}-\hat{x}_B\hat{y}_B\hat{z}_B$ is noted as $\mathscr{B}$, with its origin attached to O_{CM}, and three axes are fixed with the principal inertia axes of the formation. Body frame $O_{bi}-\hat{x}_{bi}\hat{y}_{bi}\hat{z}_{bi}$ is noted as $\mathscr{B}_i$, with its origin attached to craft-i center of mass O_{bi}, and three axes are fixed with the magnetic coils. $\mathscr{B}_i$ can be obtained by rotating $\mathscr{B}$ as 3-2-1 Euler angles $(\alpha_i, \beta_i, \gamma_i)$. Note that all the dynamics and analysis in this paper are developed in $\mathscr{B}$.

It is well known that a three-craft formation is either collinear or triangular. Actually, the collinear configuration is a special case with ϕ being equal to 0 or π, so only the relative distances are required to describe the formation geometry. Moreover, the orientation from $\mathscr{H}$ to $\mathscr{B}$ for a 1-dimension structure could be represented by only two Euler angles, while rotations around symmetric axis can be neglected with principal inertia assumption. On this account, the 6-DOF dynamic models for collinear and general triangular configurations would be developed respectively.

Before deriving the equation of motion for three-craft formation, the models of electromagnetic force and torque are introduced. Based on Ref. [16,17], the analytical far-field dipole model gives accurate results when the separation distance is many times the coil radii. Against the background of close formation flying, we use far-field dipole model to study the three-craft electromagnetic formation problem in this paper. The magnetic field on craft-i due to craft-j is defined as

$$\mathbf{B}_{ij}(\boldsymbol{\mu}_j,\ \boldsymbol{\rho}_{ij}) = \frac{\mu_0}{4\pi}\left(\frac{3\boldsymbol{\rho}_{ij}(\boldsymbol{\mu}_j\boldsymbol{\rho}_{ij})}{\rho_{ij}^5} - \frac{\boldsymbol{\mu}_j}{\rho_{ij}^3}\right) \tag{1}$$

where $\mu_0 = 4\pi \times 10^{-7}\ H/m$ is permeability of free space, $\rho_{ij} = |\boldsymbol{\rho}_{ij}| = |\boldsymbol{\rho}_j - \boldsymbol{\rho}_i|$, and $\boldsymbol{\mu}_j = [\mu_{jx} \quad \mu_{jy} \quad \mu_{jz}]^{\mathrm{T}}$. So the electromagnetic force and torque on craft-i due to craft-j can be written as

$$\begin{cases} \mathbf{F}_{ij}^{EM}(\boldsymbol{\mu}_i,\ \boldsymbol{\mu}_j,\ \boldsymbol{\rho}_{ij}) = -\frac{3\mu_0}{4\pi}\left(\frac{\boldsymbol{\mu}_i\boldsymbol{\mu}_j}{\rho_{ij}^5}\boldsymbol{\rho}_{ij} + \frac{\boldsymbol{\mu}_i\boldsymbol{\rho}_{ij}}{\rho_{ij}^5}\boldsymbol{\mu}_j + \frac{\boldsymbol{\mu}_j\boldsymbol{\rho}_{ij}}{\rho_{ij}^5}\boldsymbol{\mu}_i - 5\frac{(\boldsymbol{\mu}_i\boldsymbol{\rho}_{ij})(\boldsymbol{\mu}_j\boldsymbol{\rho}_{ij})}{\rho_{ij}^7}\boldsymbol{\rho}_{ij}\right) \\ \boldsymbol{\tau}_{ij}^{EM}(\boldsymbol{\mu}_i,\ \boldsymbol{\mu}_j,\ \boldsymbol{\rho}_{ij}) = \boldsymbol{\mu}_i \times \mathbf{B}_{ij}(\boldsymbol{\mu}_j,\ \boldsymbol{\rho}_{ij}) \end{cases} \tag{2}$$

Note that the electromagnetic force and torque applied on craft-i are due to the field interaction with all other crafts, so we can obtain

$$\mathbf{F}_i^{EM} = \mathbf{F}_{ij}^{EM} + \mathbf{F}_{ik}^{EM}, \boldsymbol{\tau}_i^{EM} = \boldsymbol{\tau}_{ij}^{EM} + \boldsymbol{\tau}_{ik}^{EM}\ (i \neq j \neq k = 1,\ 2,\ 3) \tag{3}$$

In addition, since the electromagnetic effects are internal to the formation, the electromagnetic forces applied on two crafts are equal and reverse, then $\boldsymbol{F}_{ij}^{EM} = -\boldsymbol{F}_{ji}^{EM}$. Moreover, electromagnetic force and torque cannot be used to affect the motion of the formation center of mass, and the angular momentums influenced by internal force satisfy the law of conservation, so we have

$$\sum_{i=1}^{3}(\boldsymbol{\rho}_i \times \boldsymbol{F}_i^{EM} + \boldsymbol{\tau}_i^{EM}) = 0 \tag{4}$$

2.1. Collinear formation

Similar to the study of rigid axially symmetric body under the influence of the gravity, there are three relative equilibriums for collinear three-craft electromagnetic formation, which are along the orbit radial, along-track and normal direction. In particular, our previous work on two-craft case has shown that orbit radial equilibrium and along-track equilibrium share same coupled characteristics, which is similar to the conclusion on two-craft Coulomb formation in Ref. [7]. For three-craft collinear problem, an analogous deduction could be introduced as well. On this account, we only derive the models of along-track and orbit normal configurations for simplicity.

Without loss of generality, consider a three-craft collinear configuration as shown in Fig. 1(b). From the definition of the formation center of mass, we have

$$m_1\boldsymbol{\rho}_1 + m_2\boldsymbol{\rho}_2 + m_3\boldsymbol{\rho}_3 = 0 \tag{5}$$

Thus, if once the position vectors $\boldsymbol{\rho}_1$, $\boldsymbol{\rho}_2$ are given, the vector $\boldsymbol{\rho}_3$ is also determined implicitly, so we could choose $\rho_1 = |\boldsymbol{\rho}_1| > 0$ and $\rho_2 = |\boldsymbol{\rho}_2| > 0$ to define the geometry of collinear configuration.

For the along-track configuration, the three-craft collinear formation nominally aligns with unit vector $\hat{\mathbf{y}}_B$, then

$$\boldsymbol{\rho}_1 = -\rho_1\hat{\mathbf{y}}_B, \boldsymbol{\rho}_2 = \rho_2\hat{\mathbf{y}}_B, \boldsymbol{\rho}_3 = (m_1\rho_1 - m_2\rho_2)/m_3\hat{\mathbf{y}}_B \tag{6}$$

As shown in Fig. 2(a), the (3-1) Euler angles $(\theta,\ \psi)$ are used to represent the orientation of $\mathscr{B}$ with respect to $\mathscr{H}$. As such, choose the generalized coordinates as

$$\mathbf{q} = \begin{bmatrix} q_1 & q_2 & q_3 & q_4 & q_{5,8,11} & q_{6,9,12} & q_{7,10,13} \end{bmatrix}^{\mathrm{T}} = \begin{bmatrix} \rho_1 & \rho_2 & \theta & \psi & \alpha_{1,2,3} & \beta_{1,2,3} & \gamma_{1,2,3} \end{bmatrix}^{\mathrm{T}} \tag{7}$$

Restricting our research to cases where the formation center of mass travels on a circular orbit, based on the definitions of relative orientation angles θ, ψ and relative attitude angles α_i, β_i, γ_i, we can derive the inertial velocities and angular

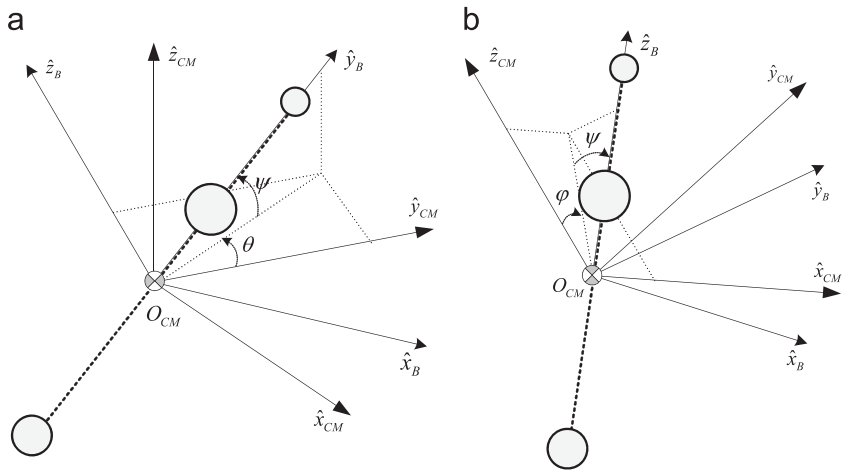

Fig. 2. Geometry of equilibrium for three-craft collinear electromagnetic formation. (a) 3-1 Euler angles for along-track equilibrium and (b) 2-1 Euler angles for orbit normal equilibrium.

velocities for each craft in terms of $\hat{\mathbf{x}}_B$, $\hat{\mathbf{y}}_B$, $\hat{\mathbf{z}}_B$, and the generalized speeds can be defined as

$$\mathbf{u}=\begin{bmatrix} u_1 & u_2 & u_3 & u_4 & u_{5,8,11} & u_{6,9,12} & u_{7,10,13}\end{bmatrix}^{\mathrm{T}}=\begin{bmatrix}\dot{\rho}_1 & \dot{\rho}_2 & \dot{\theta}+\Omega & \dot{\psi} & \omega_x^{\mathscr{B}_{1,2,3}/\mathscr{B}} & \omega_y^{\mathscr{B}_{1,2,3}/\mathscr{B}} & \omega_z^{\mathscr{B}_{1,2,3}/\mathscr{B}}\end{bmatrix}^{\mathrm{T}} \tag{8}$$

where $\Omega=\sqrt{\mu/r_{cm}^3}$ is the constant orbital rate, μ is gravity constant, r_{cm} is the radius of the circular orbit of formation center of mass, $\omega_x^{\mathscr{B}_i/\mathscr{B}}$, $\omega_y^{\mathscr{B}_i/\mathscr{B}}$, $\omega_z^{\mathscr{B}_i/\mathscr{B}}(i=1,\ 2,\ 3)$ are the components of the relative angular velocity of craft-i with respect to $\mathscr{B}$, which are defined as

$$\boldsymbol{\omega}^{\mathscr{B}_i/\mathscr{B}}=\begin{bmatrix}\omega_x^{\mathscr{B}_i/\mathscr{B}}\\ \omega_y^{\mathscr{B}_i/\mathscr{B}}\\ \omega_z^{\mathscr{B}_i/\mathscr{B}}\end{bmatrix}=\begin{bmatrix}\dot{\beta}_i\ \sin\ \alpha_i-\dot{\gamma}_i\ \cos\ \alpha_i\ \cos\ \beta_i\\ -\dot{\beta}_i\ \cos\ \alpha_i-\dot{\gamma}_i\ \sin\ \alpha_i\ \cos\ \beta_i\\ -\dot{\alpha}_i+\dot{\gamma}_i\ \sin\ \beta_i\end{bmatrix} \tag{9}$$

Additionally, after defining the partial velocities and partial angular velocities of each craft, the generalized inertia force and generalized active forces are derived based on Kane method, and the equations of motion associated with each generalized speed are obtained by setting the sum of the corresponding generalized inertia force and generalized active force as 0. The equations of motion for along-track collinear configuration of three-craft electromagnetic formation are shown as

$$\begin{cases}
\dot{u}_1=q_1(u_4^2+c_4^2u_3^2)-f_{1y}+\Sigma_y\\
\dot{u}_2=q_2(u_4^2+c_4^2u_3^2)+f_{2y}-\Sigma_y\\
\dot{u}_3=2\frac{s_4}{c_4}u_3u_4+\frac{1}{((m_1q_1-m_2q_2)^2+m_3(m_1q_1^2+m_2q_2^2))c_4}(m_3m_1q_1(f_{1x}-f_{3x})-m_3m_2q_2(f_{2x}-f_{3x})\\
\qquad +2(-m_1^2q_1+m_1m_2q_2-m_1m_3q_1)u_1u_3c_4+2(-m_2^2q_2+m_1m_2q_1-m_2m_3q_2)u_2u_3c_4)\\
\dot{u}_4=-s_4c_4u_3^2+\frac{1}{(m_1q_1-m_2q_2)^2+m_3(m_1q_1^2+m_2q_2^2)}(-m_3m_1q_1(f_{1z}-f_{3z})+m_3m_2q_2(f_{2z}-f_{3z}))\\
\qquad +2(-m_1^2q_1+m_1m_2q_2-m_1m_3q_1)u_1u_4+2(-m_2^2q_2+m_1m_2q_1-m_2m_3q_2)u_2u_4\\
\dot{u}_5=\tau_{1x}^{EM}/I_1-\dot{u}_4,\dot{u}_6=\tau_{1y}^{EM}/I_1-(\dot{u}_3s_4+u_3u_4c_4),\dot{u}_7=\tau_{1z}^{EM}/I_1-(\dot{u}_3c_4-u_3u_4s_4)\\
\dot{u}_8=\tau_{2x}^{EM}/I_2-\dot{u}_4,\dot{u}_9=\tau_{2y}^{EM}/I_2-(\dot{u}_3s_4+u_3u_4c_4),\dot{u}_{10}=\tau_{2z}^{EM}/I_2-(\dot{u}_3c_4-u_3u_4s_4)\\
\dot{u}_{11}=\tau_{3x}^{EM}/I_3-\dot{u}_4,\dot{u}_{12}=\tau_{3y}^{EM}/I_3-(\dot{u}_3s_4+u_3u_4c_4),\dot{u}_{13}=\tau_{3z}^{EM}/I_3-(\dot{u}_3c_4-u_3u_4s_4)
\end{cases} \tag{10}$$

where s_i, c_i denote $\sin\ q_i$ and $\cos\ q_i$ for short, I_i is the principal inertia of craft-i, $\mathbf{f}_i=\mathbf{f}_i^g+\mathbf{f}_i^{EM}$ is the combined acceleration of gravity and electromagnetic force applied on craft-i.

$$\Sigma_y=\frac{\mu}{M}\left(r_{cm}s_3c_4\left(\frac{m_1}{r_1^3}+\frac{m_2}{r_2^3}+\frac{m_3}{r_3^3}\right)+m_1q_1\left(\frac{1}{r_1^3}-\frac{1}{r_3^3}\right)-m_2q_2\left(\frac{1}{r_2^3}-\frac{1}{r_3^3}\right)\right) \tag{11}$$

where $M=m_1+m_2+m_3$, $r_i=|\mathbf{r}_i|$ is the inertial position length of craft-i.

For the orbital normal configuration, the unit vector $\hat{\mathbf{z}}_B$ tracks the heading of collinear configuration, choose (2–1) Euler angles $(\varphi,\ \psi)$ shown in Fig. 2(b) as the generalized coordinates $q_3,\ q_4$, and the generalized speeds $u_3,\ u_4$ are defined as $\dot{\varphi},\ \dot{\psi}$ respectively. The derivation of the equations of motion follows the same steps, and the dynamic model has a similar but more complicated formulation. Here we do not elaborate it any more.

2.2. Triangular formation

In contrast to collinear configuration, the triangular configuration as a 2-dimensional planar structure requires an additional angle $\phi \in (\pi/2, \pi)$ to define the formation geometry. As shown in Fig. 1(a), $\mathscr{B}$-frame is such defined that craft 1 is confined to axis $\hat{x}_B$ for all time, while craft 2 and 3 are aligned within $\hat{x}_B$–$\hat{y}_B$ plane, and $\mathscr{B}$ can be obtained by rotating $\mathscr{H}$ as 2-3-1 Euler angles (φ, θ, ψ). Thus, we have

$$\begin{cases} \boldsymbol{\rho}_1 = \rho_1 \hat{\mathbf{x}}_B,\ \boldsymbol{\rho}_2 = \rho_2 \cos\phi \hat{\mathbf{x}}_B - \rho_2 \sin\phi \hat{\mathbf{y}}_B \\ \boldsymbol{\rho}_3 = (-m_1/m_3\rho_1 - m_2/m_3\rho_2 \cos\phi)\hat{\mathbf{x}}_B + m_2/m_3\rho_2 \sin\phi \hat{\mathbf{y}}_B \end{cases} \tag{12}$$

In this way, we choose the generalized coordinates as

$$\mathbf{q} = \begin{bmatrix} q_1 & q_2 & q_3 & q_4 & q_5 & q_6 & q_{7,10,13} & q_{8,11,14} & q_{9,12,15} \end{bmatrix}^{\mathrm{T}} = \begin{bmatrix} \rho_1 & \rho_2 & \phi & \varphi & \theta & \psi & \alpha_{1,2,3} & \beta_{1,2,3} & \gamma_{1,2,3} \end{bmatrix}^{\mathrm{T}} \tag{13}$$

The generalized speeds can be defined as

$$\mathbf{u} = \begin{bmatrix} u_1 & u_2 & u_3 & u_4 & u_5 & u_6 & u_{7,10,13} & u_{8,11,14} & u_{9,12,15} \end{bmatrix}^{\mathrm{T}} = \begin{bmatrix} \dot{\rho}_1 & \dot{\rho}_2 & \dot{\phi} & \omega_x^{\mathscr{B}/\mathscr{N}} & \omega_y^{\mathscr{B}/\mathscr{N}} & \omega_z^{\mathscr{B}/\mathscr{N}} & \omega_x^{\mathscr{B}_{1,2,3}/\mathscr{B}} & \omega_y^{\mathscr{B}_{1,2,3}/\mathscr{B}} & \omega_z^{\mathscr{B}_{1,2,3}/\mathscr{B}} \end{bmatrix}^{\mathrm{T}} \tag{14}$$

where $\omega_x^{\mathscr{B}_i/\mathscr{B}}, \omega_y^{\mathscr{B}_i/\mathscr{B}}, \omega_z^{\mathscr{B}_i/\mathscr{B}}$ are the same as in Eq. (9), $\omega_x^{\mathscr{B}/\mathscr{N}}, \omega_y^{\mathscr{B}/\mathscr{N}}, \omega_z^{\mathscr{B}/\mathscr{N}}$ are the components of the inertial angular velocity of $\mathscr{B}$-frame, written as

$$\boldsymbol{\omega}^{\mathscr{B}/\mathscr{N}} = \begin{bmatrix} \dot{\psi} + \dot{\varphi} \sin\theta - \Omega \sin\varphi \cos\theta \\ \dot{\theta} \sin\psi + \dot{\varphi} \cos\theta \cos\psi + \Omega(\cos\varphi \sin\psi + \sin\varphi \sin\theta \cos\psi) \\ \dot{\theta} \cos\psi - \dot{\varphi} \cos\theta \sin\psi + \Omega(\cos\varphi \cos\psi - \sin\varphi \sin\theta \sin\psi) \end{bmatrix} \tag{15}$$

Finally, we can obtain the equations of motion for three-craft triangular configuration as

$$\begin{cases} \dot{u}_1 = q_1(u_5^2 + u_6^2) + f_{1x} - \Sigma_x \\ \dot{u}_2 = q_2(u_3 - u_6)^2 + q_2(u_4 s_3 + u_5 c_3)^2 + c_3(f_{2x} - \Sigma_x) - s_3(f_{2y} - \Sigma_y) \\ \dot{u}_3 = (u_4 s_3 + u_5 c_3)(u_4 c_3 - u_5 s_3) - u_4 u_5 + \frac{2u_2(u_6 - u_3)}{q_2} - \frac{2u_1 u_6}{q_1} + \frac{f_{1y} - \Sigma_y}{q_1} - \frac{s_3(f_{2x} - \Sigma_x) + c_3(f_{2y} - \Sigma_y)}{q_2} \\ \dot{u}_4 = 2\frac{c_3}{s_3} u_5 \left(\frac{u_1}{q_1} - \frac{u_2}{q_2}\right) + 2u_5 u_3 - \frac{2u_4 u_2}{q_2} - \frac{2u_4 u_3 c_3}{s_3} - u_6 u_5 - \frac{f_{2z} - \Sigma_z}{q_2 s_3} + \frac{c_3(f_{1z} - \Sigma_z)}{q_1 s_3} \\ \dot{u}_5 = -(2u_1 u_5 - q_1 u_4 u_6 + f_{1z} - \Sigma_z)/q_1 \\ \dot{u}_6 = -(2u_1 u_6 + q_1 u_4 u_5 - f_{1y} + \Sigma_z)/q_1 \\ \dot{u}_7 = \tau_{1x}^{EM}/I_1 - \dot{u}_4,\ \dot{u}_8 = \tau_{1y}^{EM}/I_1 - \dot{u}_5,\ \dot{u}_9 = \tau_{1z}^{EM}/I_1 - \dot{u}_6 \\ \dot{u}_{10} = \tau_{2x}^{EM}/I_2 - \dot{u}_4,\ \dot{u}_{11} = \tau_{2y}^{EM}/I_2 - \dot{u}_5,\ \dot{u}_{12} = \tau_{2z}^{EM}/I_2 - \dot{u}_6 \\ \dot{u}_{13} = \tau_{3x}^{EM}/I_3 - \dot{u}_4,\ \dot{u}_{14} = \tau_{3y}^{EM}/I_3 - \dot{u}_5,\ \dot{u}_{15} = \tau_{3z}^{EM}/I_3 - \dot{u}_6 \end{cases} \tag{16}$$

where $\mathbf{f}_i = \mathbf{f}_i^g + \mathbf{f}_i^{EM}$ and $r_i = |\mathbf{r}_i|$. Note they are different from the expression in Eq. (10) due to the varied rotating matrix from $\mathscr{H}$ to $\mathscr{B}$, and

$$\boldsymbol{\Sigma} = \begin{bmatrix} \Sigma_x \\ \Sigma_y \\ \Sigma_z \end{bmatrix} = -\frac{\mu}{M} \begin{bmatrix} r_{cm} c_4 c_5 (m_1/r_1^3 + m_2/r_2^3 + m_3/r_3^3) + m_1 q_1 (1/r_1^3 - 1/r_3^3) + m_2 q_2 c_3 (1/r_2^3 - 1/r_3^3) \\ r_{cm}(s_4 s_6 - c_4 s_5 c_6)(m_1/r_1^3 + m_2/r_2^3 + m_3/r_3^3) - m_2 q_2 s_3 (1/r_2^3 - 1/r_3^3) \\ r_{cm}(s_4 c_6 + c_4 s_5 s_6)(m_1/r_1^3 + m_2/r_2^3 + m_3/r_3^3) \end{bmatrix} \tag{17}$$

So far, we have obtained the 6-DOF nonlinear dynamic models of three-craft electromagnetic formation for collinear and general triangular configuration respectively. By examining the formulations of these models, it is obvious that the system dynamics has complicated nonlinear and coupled characteristics. The nonlinearities embody in electromagnetic force model and the terms of trigonometric function, and the coupled characteristics are dependent on the coupled relative trajectory/attitude motion and coupled electromagnetic force/torque model.

3. Shape solutions of static configurations

The invariant shape studied in this paper is confined to a fixed configuration that maintains the formation geometry all along with real and constant magnetic moments. Naturally, it follows a static or spinning configuration. For the static configuration, the crafts appear stationary or frozen with respect to $\mathscr{H}$-frame, and all state variables take on constant values, corresponding to the relative equilibrium of the dynamic model. In the following sections, we would like to study the invariant shape solutions for static collinear and triangular configurations respectively.

3.1. Static collinear configuration

Substituting the relative equilibrium conditions $\dot{\bar{\mathbf{q}}}=0, \dot{\bar{\mathbf{u}}}=0$ into Eq. (10), where the superscript "−" is used to denote the equilibrium state, we can obtain

$$\bar{\boldsymbol{\tau}}_i^{EM}=\begin{bmatrix}\bar{\tau}_{ix}^{EM} & \bar{\tau}_{iy}^{EM} & \bar{\tau}_{iz}^{EM}\end{bmatrix}^{\mathrm{T}}=0 \tag{18}$$

It is apparent that the electromagnetic torques applied to all crafts are zero in the static collinear configuration. Indeed, in order to determine the possible invariant shapes, the feasible magnetic moment solutions satisfying Eq. (18) should be examined first, then comes to identify whether the families of invariant shape solutions do exit with given magnetic moments by checking other equilibrium conditions.

3.1.1. Along-track

For the along-track collinear configuration, substituting $\boldsymbol{\rho}_{ij}=\rho_{ij}\hat{\mathbf{y}}_B$ into Eq. (1) yields

$$\mathbf{B}_{ij}=\frac{\mu_0}{4\pi\rho_{ij}^3}\begin{bmatrix}-\mu_{jx} & 2\mu_{jy} & -\mu_{jz}\end{bmatrix}^{\mathrm{T}} \tag{19}$$

Considering $\boldsymbol{\tau}_i^{EM}=\boldsymbol{\mu}_i\times(\mathbf{B}_{ij}+\mathbf{B}_{ik})$, three possible cases are examined to satisfy Eq. (18).

Case A: $\bar{\boldsymbol{\mu}}_i=0$

In order to ensure the electromagnetic effect, at least two of magnetic moments should not be zero. When $\bar{\boldsymbol{\mu}}_i=0$, we have $\bar{\mathbf{B}}_{ji}=\bar{\mathbf{B}}_{ki}=0$, then $\bar{\boldsymbol{\tau}}_j^{EM}=\bar{\boldsymbol{\mu}}_j\times\bar{\mathbf{B}}_{jk}=0$ and $\bar{\boldsymbol{\tau}}_k^{EM}=\bar{\boldsymbol{\mu}}_k\times\bar{\mathbf{B}}_{kj}=0$, which are expanded with components formulation to give

$$\bar{\mu}_{jy}\bar{\mu}_{kz}+\bar{\mu}_{ky}\bar{\mu}_{jz}=0,\ \bar{\mu}_{jx}\bar{\mu}_{ky}+\bar{\mu}_{kx}\bar{\mu}_{jy}=0,\ \bar{\mu}_{jx}\bar{\mu}_{kz}=\bar{\mu}_{kx}\bar{\mu}_{jz} \tag{20}$$

Hence the electromagnetic effect only occurs between craft-j and craft-k, and the inter-craft electromagnetic force is aligned with axis $\hat{y}_B$.

Case B: $\bar{\mathbf{B}}_{ij}+\bar{\mathbf{B}}_{ik}=0$

When $\bar{\mathbf{B}}_{ij}=-\bar{\mathbf{B}}_{ik}$, we obtain $\bar{\boldsymbol{\mu}}_j=-\bar{\rho}_{ij}^3/\bar{\rho}_{ki}^3\bar{\boldsymbol{\mu}}_k$ based on Eq. (19). Moreover, we can derive $\bar{\mathbf{B}}_{kj}=-\bar{\rho}_{ij}^3/\bar{\rho}_{ik}^3\bar{\mathbf{B}}_{jk}$ and $\bar{\mathbf{B}}_{ki}=\bar{\rho}_{ij}^3/\bar{\rho}_{ki}^3\bar{\mathbf{B}}_{ji}$, so

$$\begin{cases}\bar{\boldsymbol{\tau}}_j^{EM}=-\bar{\rho}_{ij}^3/\bar{\rho}_{ki}^3\bar{\boldsymbol{\mu}}_k\times(\bar{\mathbf{B}}_{ji}+\bar{\mathbf{B}}_{jk})=0\\ \bar{\boldsymbol{\tau}}_k^{EM}=\bar{\rho}_{ij}^3/\bar{\rho}_{ki}^3\bar{\boldsymbol{\mu}}_k\times(\bar{\mathbf{B}}_{ji}-\bar{\mathbf{B}}_{jk})=0\end{cases}\Rightarrow\begin{cases}\bar{\boldsymbol{\mu}}_k\times\bar{\mathbf{B}}_{ji}=0\\ \bar{\boldsymbol{\mu}}_k\times\bar{\mathbf{B}}_{jk}=0\end{cases} \tag{21}$$

which are expanded with components formulation as

$$\begin{cases}-2\bar{\mu}_{iy}\bar{\mu}_{kz}-\bar{\mu}_{ky}\bar{\mu}_{iz}=0\\ \bar{\mu}_{kx}\bar{\mu}_{iz}-\bar{\mu}_{ix}\bar{\mu}_{kz}=0\\ \bar{\mu}_{ix}\bar{\mu}_{ky}+2\bar{\mu}_{kx}\bar{\mu}_{iy}=0\end{cases},\ \begin{cases}-3\bar{\mu}_{ky}\bar{\mu}_{kz}=0\\ 3\bar{\mu}_{kx}\bar{\mu}_{ky}=0\end{cases} \tag{22}$$

Next, discuss the conditions satisfying Eq. (22) besides $\bar{\boldsymbol{\mu}}_k=0$ which has been analyzed in Case A. (i) If $\bar{\mu}_{ky}=0$ and $\bar{\mu}_{kx}$, $\bar{\mu}_{kz}$ are not simultaneously zero, $\bar{\mu}_{iy}=0$ and $\bar{\mu}_{kx}\bar{\mu}_{iz}=\bar{\mu}_{ix}\bar{\mu}_{kz}$ should be required. So the y components of $\bar{\boldsymbol{\mu}}_i$, $\bar{\boldsymbol{\mu}}_k$ are both zero, and come with $\bar{\boldsymbol{\mu}}_i//\bar{\boldsymbol{\mu}}_k$. (ii) If $\bar{\mu}_{ky}\neq0$ and $\bar{\mu}_{kx}=\bar{\mu}_{kz}=0$, $\bar{\mu}_{ix}=\bar{\mu}_{iz}=0$ is required, which means that only the y components of $\bar{\boldsymbol{\mu}}_i$, $\bar{\boldsymbol{\mu}}_k$ are not zero, and $\bar{\boldsymbol{\mu}}_i//\bar{\boldsymbol{\mu}}_k$ is true as well.

Therefore, the magnetic moments of three crafts must be parallel with each other, and either the y components are zero or the x, z components are both zero. Thus, we can define $\bar{\boldsymbol{\mu}}_j=-\bar{\rho}_{ij}^3/\bar{\rho}_{ki}^3\bar{\boldsymbol{\mu}}_k$ and $\boldsymbol{\mu}_i=\lambda\boldsymbol{\mu}_k$, where λ is a proportionality coefficient to be determined.

Case C: $\bar{\boldsymbol{\mu}}_i//(\bar{\mathbf{B}}_{ij}+\bar{\mathbf{B}}_{ik})$

Considering the instance when $\bar{\boldsymbol{\mu}}_i//(\bar{\mathbf{B}}_{ij}+\bar{\mathbf{B}}_{ik})$ is true for all three crafts, we can rewrite the formulation as

$$\begin{cases}\bar{\boldsymbol{\mu}}_1=l'_1(\bar{\mathbf{B}}_{12}+\bar{\mathbf{B}}_{13})=l_1\left(\frac{3\bar{\mu}_{2y}}{\bar{\rho}_{12}^3}\hat{\mathbf{y}}_B-\frac{\bar{\boldsymbol{\mu}}_2}{\bar{\rho}_{12}^3}+\frac{3\bar{\mu}_{3y}}{\bar{\rho}_{31}^3}\hat{\mathbf{y}}_B-\frac{\bar{\boldsymbol{\mu}}_3}{\bar{\rho}_{31}^3}\right)\\ \bar{\boldsymbol{\mu}}_2=l'_2(\bar{\mathbf{B}}_{21}+\bar{\mathbf{B}}_{23})=l_2\left(\frac{3\bar{\mu}_{1y}}{\bar{\rho}_{12}^3}\hat{\mathbf{y}}_B-\frac{\bar{\boldsymbol{\mu}}_1}{\rho_{12}^3}+\frac{3\bar{\mu}_{3y}}{\rho_{23}^3}\hat{\mathbf{y}}_B-\frac{\bar{\boldsymbol{\mu}}_3}{\bar{\rho}_{23}^3}\right)\\ \bar{\boldsymbol{\mu}}_3=l'_3(\bar{\mathbf{B}}_{31}+\bar{\mathbf{B}}_{32})=l_3\left(\frac{3\bar{\mu}_{1y}}{\bar{\rho}_{31}^3}\hat{\mathbf{y}}_B-\frac{\bar{\boldsymbol{\mu}}_1}{\rho_{31}^3}+\frac{3\bar{\mu}_{2y}}{\rho_{23}^3}\hat{\mathbf{y}}_B-\frac{\bar{\boldsymbol{\mu}}_2}{\bar{\rho}_{23}^3}\right)\end{cases} \tag{23}$$

where $l_i(i=1,2,3)$ are proportionality coefficients, which can be determined by making equal of corresponding coefficients of $\bar{\boldsymbol{\mu}}_i$. Accordingly, the relations between magnetic moments are given as

$$\begin{cases}\bar{\boldsymbol{\mu}}_1+\bar{\rho}_{31}^3/\bar{\rho}_{23}^3\bar{\boldsymbol{\mu}}_2+\bar{\rho}_{12}^3/\bar{\rho}_{23}^3\bar{\boldsymbol{\mu}}_3=6\bar{\mu}_{1y}\hat{\mathbf{y}}_B\\ \bar{\mu}_{1y}=\bar{\rho}_{31}^3/\bar{\rho}_{23}^3\bar{\mu}_{2y}=\bar{\rho}_{12}^3/\bar{\rho}_{23}^3\bar{\mu}_{3y}\end{cases}\Rightarrow\begin{cases}\bar{\mu}_{1x}+\bar{\rho}_{31}^3/\bar{\rho}_{23}^3\bar{\mu}_{2x}+\bar{\rho}_{12}^3/\bar{\rho}_{23}^3\bar{\mu}_{3x}=0\\ \bar{\mu}_{1y}=\bar{\mu}_{2y}=\bar{\mu}_{3y}=0\\ \bar{\mu}_{1z}+\bar{\rho}_{31}^3/\bar{\rho}_{23}^3\bar{\mu}_{2z}+\bar{\rho}_{12}^3/\bar{\rho}_{23}^3\bar{\mu}_{3z}=0\end{cases} \tag{24}$$

Therefore, the magnetic moments of three crafts should satisfy the linear relation shown in Eq. (24), and the y components are both equal to zero.

Based on the above analysis, the possible shape solutions for each case are identified. When the along-track collinear configuration achieves relative static equilibrium, $\mathscr{B}$-frame coincides with $\mathscr{H}$ to give $\bar{q}_3=\bar{q}_4=0$, and thus $\bar{u}_3=\Omega$, $\bar{u}_i=0(i\neq 3)$. Substituting $\dot{\bar{\mathbf{q}}}=0$, $\dot{\bar{\mathbf{u}}}=0$ and Eq. (4) for along-track configuration into the equations of motion Eq. (16), we obtain

$$\begin{cases} \bar{q}_1\Omega^2-\mu\bar{q}_1/\bar{r}_1^3-\left(\bar{F}_{12y}^{EM}-\bar{F}_{31y}^{EM}\right)/m_1=0 \\ \bar{q}_2\Omega^2-\mu\bar{q}_2/\bar{r}_2^3+\left(\bar{F}_{23y}^{EM}-\bar{F}_{12y}^{EM}\right)/m_2=0 \\ m_1\bar{q}_1\left(1/\bar{r}_1^3-1/\bar{r}_3^3\right)=m_2\bar{q}_2\left(1/\bar{r}_2^3-1/\bar{r}_3^3\right) \end{cases} \tag{25}$$

where $\bar{r}_1=\sqrt{r_{cm}^2+\bar{q}_1^2}$, $\bar{r}_2=\sqrt{r_{cm}^2+\bar{q}_2^2}$, $\bar{r}_3=\sqrt{r_{cm}^2+\left(m_1\bar{q}_1-m_2\bar{q}_2\right)^2/m_3^2}$.

For case A, let $\bar{\boldsymbol{\mu}}_1=0$, so all the inter-craft electromagnetic forces are zero except for F_{23y}^{EM} which is approximate to 0. By inspection, it is evident that craft 1 is located at the formation center of mass for $\bar{q}_1=0$, while craft 2 and 3 are located at right and left side in the formation. Moreover, $\bar{r}_2=\bar{r}_3$ is required from the third equation of Eq. (25), which implies $m_2=m_3$ and $\bar{q}_2=\bar{\rho}_3$. Thus, craft 2 and craft 3 in along-track collinear equilibrium are of equal mass and located of equal distance. Note that we omit the derivation when either $\bar{\boldsymbol{\mu}}_2$ or $\bar{\boldsymbol{\mu}}_3$ is zero since the procedure is similar and conclusion same. Actually, such formations are similar to the two-craft electromagnetic formation, and the shape solutions are the same too. In particular, assuming the magnetic moment of the two crafts both being $\bar{\boldsymbol{\mu}}=\bar{\mu}_y\hat{\mathbf{y}}_B$, we can solve

$$\bar{\mu}_y=\sqrt{32\pi\bar{q}^4\bar{F}_y^{EM}/3\mu_0}\approx 0 \tag{26}$$

For case B, assume the magnetic moments of crafts satisfy $\bar{\boldsymbol{\mu}}_1=\lambda\bar{\boldsymbol{\mu}}_3$, $\bar{\boldsymbol{\mu}}_2=-\bar{\rho}_{12}^3/\bar{\rho}_{31}^3\bar{\boldsymbol{\mu}}_3$ with $\bar{\mu}_{iy}=0$ or $\bar{\mu}_{ix}=\bar{\mu}_{iz}=0$, thus the inter-craft electromagnetic forces can be given as

$$\begin{cases} \bar{\mathbf{F}}_{12}^{EM}=\frac{3\mu_0(\bar{\mu}_{3x}^2+\bar{\mu}_{3z}^2)\lambda}{4\pi(\bar{q}_1+\bar{q}_2)(\bar{q}_1+\bar{\rho}_3)^3}\hat{\mathbf{y}}_B \\ \bar{\mathbf{F}}_{23}^{EM}=\frac{3\mu_0(\bar{\mu}_{3x}^2+\bar{\mu}_{3z}^2)(\bar{q}_1+\bar{q}_2)^3}{4\pi(\bar{q}_1+\bar{\rho}_3)^3(\bar{q}_2-\bar{\rho}_3)^4}\hat{\mathbf{y}}_B \\ \bar{\mathbf{F}}_{31}^{EM}=\frac{3\mu_0(\bar{\mu}_{3x}^2+\bar{\mu}_{3z}^2)\lambda}{4\pi(\bar{q}_1+\bar{\rho}_3)^4}\hat{\mathbf{y}}_B \end{cases} \text{ or } \begin{cases} \bar{\mathbf{F}}_{12}^{EM}=-\frac{3\mu_0\bar{\mu}_{3y}^2\lambda}{2\pi(\bar{q}_1+\bar{q}_2)(\bar{q}_1+\bar{\rho}_3)^3}\hat{\mathbf{y}}_B \\ \bar{\mathbf{F}}_{23}^{EM}=-\frac{3\mu_0\bar{\mu}_{3y}^2(\bar{q}_1+\bar{q}_2)^3}{2\pi(\bar{q}_1+\bar{\rho}_3)^3(\bar{q}_2-\bar{\rho}_3)^4}\hat{\mathbf{y}}_B \\ \bar{\mathbf{F}}_{31}^{EM}=-\frac{3\mu_0\bar{\mu}_{3y}^2\lambda}{2\pi(\bar{q}_1+\bar{\rho}_3)^4}\hat{\mathbf{y}}_B \end{cases} \tag{27}$$

Since the distance ρ_i is minor relative to r_{cm}, using first order Taylor series approximation on $1/\bar{r}_i^3$, and ignoring the higher order terms of ρ_i/r_{cm}, we can derive $\bar{F}_{12y}^{EM}\approx\bar{F}_{31y}^{EM}\approx\bar{F}_{23y}^{EM}$. An examination of Eq. (27) shows that $\bar{q}_2=\bar{\rho}_3$ must be true, which means that craft 2 and 3 coincide with each other. Such formation is impossible to achieve, thus there is no feasible shape solution for case B.

For case C, assume magnetic moment of craft 1 is $\bar{\boldsymbol{\mu}}_1=-\bar{\rho}_{31}^3/\bar{\rho}_{23}^3\bar{\boldsymbol{\mu}}_2-\bar{\rho}_{12}^3/\bar{\rho}_{23}^3\bar{\boldsymbol{\mu}}_3$ for given $\bar{\boldsymbol{\mu}}_2$, $\bar{\boldsymbol{\mu}}_3$ with $\bar{\mu}_{iy}=0$, then the inter-craft electromagnetic forces can be given as

$$\begin{cases} \bar{\mathbf{F}}_{12}^{EM}=-\frac{3\mu_0\left((\bar{\mu}_{2x}\bar{\mu}_{3x}+\bar{\mu}_{2z}\bar{\mu}_{3z})(\bar{q}_1+\bar{q}_2)^3+(\bar{\mu}_{2x}^2+\bar{\mu}_{2z}^2)(\bar{q}_1+\bar{\rho}_3)^3\right)}{4\pi(\bar{q}_1+\bar{q}_2)^4(\bar{q}_2-\bar{\rho}_3)^3}\hat{\mathbf{y}}_B \\ \bar{\mathbf{F}}_{23}^{EM}=-\frac{3\mu_0(\bar{\mu}_{2x}\bar{\mu}_{3x}+\bar{\mu}_{2z}\bar{\mu}_{3z})}{4\pi(\bar{q}_2-\bar{\rho}_3)^4}\hat{\mathbf{y}}_B \\ \bar{\mathbf{F}}_{31}^{EM}=\frac{3\mu_0\left((\bar{\mu}_{2x}\bar{\mu}_{3x}+\bar{\mu}_{2z}\bar{\mu}_{3z})(\bar{q}_1+\bar{\rho}_3)^3+(\bar{\mu}_{3x}^2+\bar{\mu}_{3z}^2)(\bar{q}_1+\bar{q}_2)^3\right)}{4\pi(\bar{q}_1+\bar{\rho}_3)^4(\bar{q}_2-\bar{\rho}_3)^3}\hat{\mathbf{y}}_B \end{cases} \tag{28}$$

In the same way, based on $\bar{F}_{12y}^{EM}\approx\bar{F}_{31y}^{EM}\approx\bar{F}_{23y}^{EM}$, we have

$$(\bar{\mu}_{2x}^2+\bar{\mu}_{2z}^2)/(\bar{\mu}_{3x}^2+\bar{\mu}_{3z}^2)=-((\bar{q}_1+\bar{q}_2)/(\bar{q}_1+\bar{\rho}_3))^5>0 \tag{29}$$

which depicts families of invariant shape solutions under case C where craft 3 is located at leftmost of the formation since $\bar{q}_1+\bar{\rho}_3<0$ must be true for all time. In particular, we can obtain a special shape while $\bar{\boldsymbol{\mu}}_2=\bar{\boldsymbol{\mu}}_3$ as

$$\bar{\rho}_3=-2\bar{q}_1-\bar{q}_2\Rightarrow(m_1+2m_3)\bar{q}_1=(m_2-m_3)\bar{q}_2 \tag{30}$$

Since $m_i>0$ and $\bar{q}_i>0$, the shape solutions of Eq. (30) are permissible only when $m_2>m_3$ is true for all time, which can be solved for given m_i.

3.1.2. Orbit normal

For the orbit normal collinear configuration, the relative static equilibrium follows the same conditions except for $\overline{u}_i = 0$, thus the equilibrium equations of motion are derived as

$$\begin{cases} -\mu\overline{q}_1/\overline{r}_1^3 - (\overline{F}_{12z}^{EM} - \overline{F}_{31z}^{EM})/m_1 = 0 \\ -\mu\overline{q}_2/\overline{r}_2^3 + (\overline{F}_{23z}^{EM} - \overline{F}_{12z}^{EM})/m_2 = 0 \\ m_1\overline{q}_1(1/\overline{r}_1^3 - 1/\overline{r}_3^3) = m_2\overline{q}_2(1/\overline{r}_2^3 - 1/\overline{r}_3^3) \end{cases} \tag{31}$$

where $\overline{r}_i$ are same as the expressions in Eq. (25).

Again, using first order Taylor series approximation on Eq. (31), and ignoring the higher order terms of ρ_i/r_{cm}, we can derive

$$\begin{cases} \overline{F}_{12z}^{EM} - \overline{F}_{31z}^{EM} \approx -\mu m_1\overline{q}_1/r_{cm}^3 < 0 \\ \overline{F}_{12z}^{EM} - \overline{F}_{23z}^{EM} \approx -\mu m_2\overline{q}_2/r_{cm}^3 < 0 \end{cases} \tag{32}$$

Substituting $\boldsymbol{\rho}_{ij} = \rho_{ij}\hat{\mathbf{z}}_B$ and following the derivation shown in Section 3.1.1, it concludes that the feasible magnetic moment solutions satisfying Eq. (18) for orbit normal configurations have a similar formulation. Here we would identify the possible invariant shape solutions directly.

For case A, we assume $\overline{\boldsymbol{\mu}}_3 = 0$ without loss of generality, then all the inter-electromagnetic forces are zero except $\overline{F}_{12y}^{EM}$ which is a repulsive force to maintain the formation. From Eq. (31) $m_1\overline{q}_1 = m_2\overline{q}_2$ is derived, which means that craft 3 is located at the formation center of mass. Moreover $\overline{q}_1 = \overline{q}_2$ and $m_1 = m_2$ are required, which imply that craft 1 and 2 are located at left and right side in the formation with equal mass and equal distance. Similarly, when $\overline{\boldsymbol{\mu}}_1 = \overline{\boldsymbol{\mu}}_2 = \mu_z\hat{\mathbf{z}}_B$, the equilibrium magnetic moment is written as

$$\overline{\mu}_z = \sqrt{-32\pi\overline{q}^4\overline{F}_z^{EM}/3\mu_0} \approx \sqrt{32\pi\Omega^2 m\overline{q}^5/3\mu_0} \tag{33}$$

For case B, the magnetic moments of crafts satisfy $\overline{\boldsymbol{\mu}}_i = \lambda\overline{\boldsymbol{\mu}}_k$, $\overline{\boldsymbol{\mu}}_j = -\overline{\rho}_{ij}^3/\overline{\rho}_{ki}^3\overline{\boldsymbol{\mu}}_k$ with $\overline{\mu}_{iz} = 0$ or $\overline{\mu}_{ix} = \overline{\mu}_{iy} = 0$. Given $\overline{\boldsymbol{\mu}}_3$, the inter-craft electromagnetic forces share a same expression with Eq. (27) except for replacing $\hat{\mathbf{y}}_B$ by $-\hat{\mathbf{z}}_B$. Thus the proportionality coefficient λ can be determined by examining Eq. (32) as

$$\lambda = \frac{m_1\overline{q}_1(\overline{q}_1 + \overline{\rho}_3)(\overline{q}_1 + \overline{q}_2)^4}{(\overline{q}_2 - \overline{\rho}_3)^4(m_2\overline{q}_2(\overline{q}_2 - \overline{\rho}_3) + m_1\overline{q}_1(\overline{q}_1 + \overline{\rho}_3))} \tag{34}$$

Therefore, $\overline{q}_2 \neq \overline{\rho}_3$ is required to offer a feasible solution. Note that the denominator in Eq. (34) has been checked as true for any collinear geometry.

For case C, the magnetic moments of crafts satisfy $\overline{\boldsymbol{\mu}}_1 + \overline{\rho}_{31}^3/\overline{\rho}_{23}^3\overline{\boldsymbol{\mu}}_2 + \overline{\rho}_{12}^3/\overline{\rho}_{23}^3\overline{\boldsymbol{\mu}}_3 = 0$ with $\overline{\mu}_{iz} = 0$, and the electromagnetic forces are the same as the expression in Eq. (28) except for replacing $\hat{\mathbf{y}}_B$ by $-\hat{\mathbf{z}}_B$. Similarly, we can derive the relationship

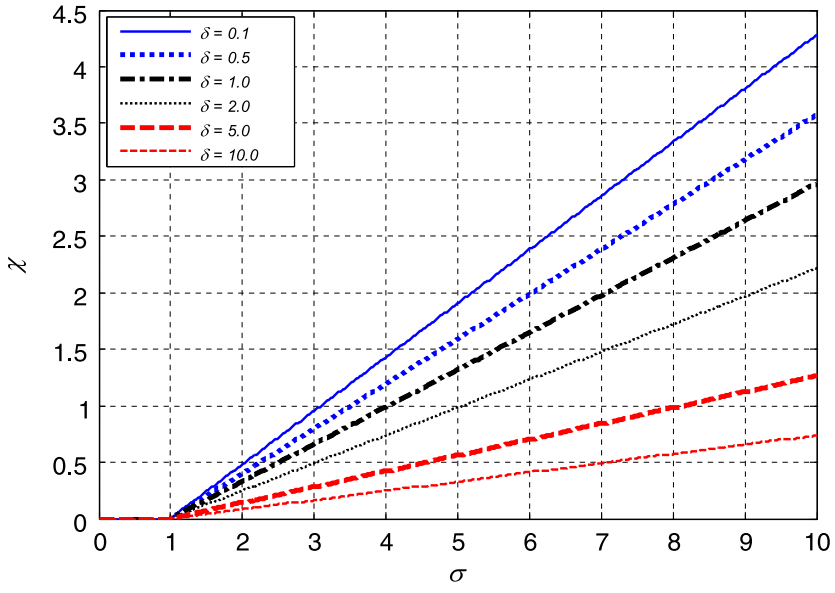

Fig. 3. Special shape solutions for orbit normal configuration.

between the formation geometry and magnetic moments as

$$\frac{m_3\bar{\rho}_3}{m_2\bar{q}_2}=\frac{(\bar{q}_1+\bar{q}_2)^5}{(\bar{q}_1+\bar{\rho}_3)^5}\cdot\frac{(\mu_{3x}^2+\mu_{3y}^2)(\bar{q}_1+\bar{q}_2)^2(\bar{q}_2-\bar{\rho}_3)+(\mu_{2x}\mu_{3x}+\mu_{2y}\mu_{3y})(\bar{q}_1+\bar{\rho}_3)^3}{(\mu_{2x}^2+\mu_{2y}^2)(\bar{q}_1+\bar{\rho}_3)^2(\bar{q}_2-\bar{\rho}_3)-(\mu_{2x}\mu_{3x}+\mu_{2y}\mu_{3y})(\bar{q}_1+\bar{q}_2)^3} \tag{35}$$

In particular, let $\chi=\bar{q}_1/\bar{q}_2$, $\delta=m_1/m_3$ and $\sigma=m_2/m_3$, which are all positive real number. Thus, we can obtain the special shapes while $\bar{\boldsymbol{\mu}}_2=\bar{\boldsymbol{\mu}}_3$ as

$$\frac{\delta\chi-\sigma}{\sigma}=\frac{(\chi+1)^5\quad(\chi+1)^2(1-\delta\chi+\sigma)+(\chi+\delta\chi-\sigma)^3}{(\chi+\delta\chi-\sigma)^5\,(\chi+\delta\chi-\sigma)^2(1-\delta\chi+\sigma)-(\chi+1)^3} \tag{36}$$

Eq. (36) is a polynomial equation about χ, which can be determined by given δ, σ. According to the definition of χ, each solution to this equation gives a family of invariant shape solutions for such collinear formation. The values of χ with varied δ, σcan be seen in Fig. 3. Numerically simulation shows that for any given δ, $\sigma>0$, there exists at most one solution for χ to satisfy Eq. (36), and there is no feasible shape solution while $\sigma<1$.

3.2. Static triangular configuration

Unlike the collinear configuration, the equilibrium torque conditions for the triangular configuration are too nonlinear to get an analytical formulation, hence it is very difficult to examine the feasible magnetic moments solutions. In Ref. [16] Schweighart presented two numerical algorithms by Newton's method and continuation method to solve the polynomial equations about magnetic dipoles. However, one can check some special invariant shape solutions do exist. Here we first examine the appropriate configuration constraints based on angular momentum conservation, and then identify the feasible magnetic moment solutions for special formation geometry meeting the equilibrium conditions.

When the triangular configuration achieves the relative static equilibrium, the electromagnetic torques satisfy Eq. (18) as well, so the expression for angular momentum conservation is derived as

$$\begin{cases} 0=\bar{f}_{2z}^{EM}-\bar{f}_{3z}^{EM},\ 0=\bar{f}_{1z}^{EM}-\bar{f}_{3z}^{EM} \\ 0=m_1\bar{q}_1(\bar{f}_{1y}^{EM}-\bar{f}_{3y}^{EM})+m_2\bar{q}_2c_3(\bar{f}_{2y}^{EM}-\bar{f}_{3y}^{EM})+m_2\bar{q}_2s_3(\bar{f}_{2x}^{EM}-\bar{f}_{3x}^{EM}) \end{cases} \tag{37}$$

Previous work has shown that axis $\hat{z}_B$ of an arbitrary triangular electromagnetic formation must align with one of three $\mathscr{H}$-frame axes to satisfy relative static equilibrium, which is similar to Coulomb formation in Ref. [6]. In addition, given the similar geometry and mechanics characteristics between the cases of $\hat{z}_B$ axis along orbit normal and along-track direction, we only consider the two cases where three crafts are coplanar with the orbital plane or perpendicular to radial direction here.

For the triangular static electromagnetic formation lying in the orbital plane, $\mathscr{B}$-frame coincides with $\mathscr{H}$-frame to give $\bar{q}_4=\bar{q}_5=\bar{q}_6=0$, and thus $\bar{u}_i$ are all equal to zero except for $\bar{u}_6=\Omega$. The equilibrium acceleration of electromagnetic force can be derived from Eq. (16) at relative equilibrium. After checking the conditions in Eq. (37), we obtain

$$\bar{r}_2=\bar{r}_3\Rightarrow 2m_3r_{cm}(m_1\bar{q}_1+(m_2+m_3)\bar{q}_2c_3)=2m_1m_2\bar{q}_1\bar{q}_2c_3+m_1^2\bar{q}_1^2+m_2^2\bar{q}_2^2-m_3^2\bar{q}_2^2 \tag{38}$$

It is obvious that craft 2 and craft 3 must be located equally distant to the center of earth. In particular, when $m_1\bar{q}_1+(m_2+m_3)\bar{q}_2c_3=0$, the projections of $\bar{\boldsymbol{\rho}}_2$, $\bar{\boldsymbol{\rho}}_3$ along axis $\hat{x}_B$ have equal value, and $m_2=m_3$ is derived from Eq. (38) as well. So far, the three-craft formation geometry should be a radially symmetrical isosceles triangle. A same conclusion for three-craft formation perpendicular to along-track direction can also be obtained.

For the triangular configuration perpendicular to radial direction, the formation maintains relative static equilibrium with axis $\hat{z}_B$ aligned with radial direction. Let $\bar{q}_4=\pi/2$, $\bar{q}_5=\bar{q}_6=0$, and thus $\bar{u}_i$ are all equal to zero except for $\bar{u}_4=-\Omega$. Following the similar procedures, we obtain

$$\begin{cases} \bar{r}_1=\bar{r}_2=\bar{r}_3 \\ m_1\bar{q}_1+(m_2+m_3)\bar{q}_2c_3=0 \end{cases}\Rightarrow\begin{cases} \bar{q}_1=\bar{q}_2 \\ 2m_1m_2c_3=m_3^2-m_1^2-m_2^2 \end{cases} \tag{39}$$

which means that the distances of all three crafts relative to the center of earth must be equal, constituting an isosceles triangle. Furthermore, based on geometrical symmetry about axis $\hat{x}_B$, $m_2=m_3$ is necessary to make $\bar{\rho}_{2y}=\bar{\rho}_{3y}$ true.

In both cases, an isosceles triangle configuration can always be found to maintain static formation relative to $\mathscr{H}$ for all time, and such shape constraints represent sufficient conditions with the existence of feasible magnetic moment solutions unknown yet. To explore the magnetic moment solutions, we revisit Eq. (37) and find all three accelerations of electromagnetic force along axis $\hat{z}_B$ to be equal, then $\bar{F}_{12z}^{EM}=\bar{F}_{23z}^{EM}=\bar{F}_{31z}^{EM}$ can be ensured. Since the resulting equations are far too complex, $\bar{\mu}_{iz}=0$ as a special solution is checked to meet the condition and make $\bar{F}_{iz}^{EM}=0$. Next, the magnetic moment solutions would be identified under such circumstances.

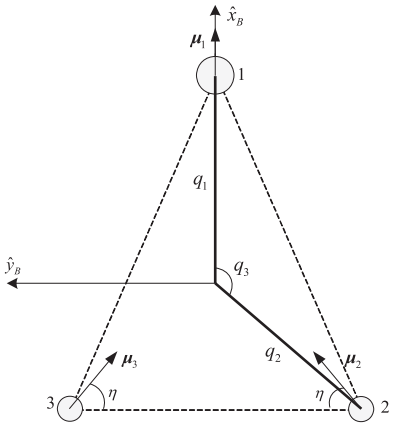

Fig. 4. Magnetic moments for three-craft triangular static configuration.

Considering the triangular configuration with $\bar{q}_1=\bar{q}_2=\bar{q}$, $m_2=m_3$ and $c_3=-m_1/2m_2$, the required accelerations of electromagnetic force for the case of three-craft formation perpendicular to radial direction are derived as

$$\begin{cases}\bar{f}_{1x}^{EM}=\mu\bar{q}/\bar{r}_1^3\\ \bar{f}_{1y}^{EM}=0\end{cases},\ \begin{cases}\bar{f}_{2x}^{EM}=\mu\bar{q}c_3/\bar{r}_1^3=c_3\bar{f}_{1x}^{EM}\\ \bar{f}_{2y}^{EM}=\bar{q}s_3\Omega^2-\mu\bar{q}s_3/\bar{r}_1^3\approx 0\end{cases},\ \begin{cases}\bar{f}_{3x}^{EM}=\bar{f}_{2x}^{EM}\\ \bar{f}_{3y}^{EM}=-\bar{f}_{2y}^{EM}\end{cases} \tag{40}$$

where $\bar{r}_1=\sqrt{r_{cm}^2+\bar{q}^2}$, $\bar{r}_2=\bar{r}_3=\bar{r}_1$. For the case of three crafts lying in the orbital plane, we can obtain a similar formulation by using first order Taylor series approximation, which is examined to satisfy the same relationship in Eq. (40). In this manner, craft 1 is exerting repulsive forces on other two crafts, and attractive force is required between craft 2 and 3, or both reverse. Therefore, the electromagnetic forces applied on all three crafts are symmetrical about axis $\hat{x}_B$, and the magnetic moments of three crafts should be symmetric accordingly.

As shown in Fig. 4, assume the magnetic moments for each craft as

$$\bar{\boldsymbol{\mu}}_1=\begin{bmatrix}\bar{\mu}_1 & 0 & 0\end{bmatrix}^{\mathrm{T}},\bar{\boldsymbol{\mu}}_2=\begin{bmatrix}\bar{\mu}_2\ \sin\eta & \bar{\mu}_2\ \cos\eta & 0\end{bmatrix}^{\mathrm{T}},\ \bar{\boldsymbol{\mu}}_3=\begin{bmatrix}\bar{\mu}_3\ \sin\eta & -\bar{\mu}_3\ \cos\eta & 0\end{bmatrix}^{\mathrm{T}} \tag{41}$$

where $\bar{\mu}_i$ is magnitude of $\bar{\boldsymbol{\mu}}_i$, and $\eta\in(0,\pi/2)$ is the angle between $\bar{\boldsymbol{\mu}}_i$ and axis $\hat{y}_B$. By substituting Eq.(41) into $\bar{\boldsymbol{\tau}}_i^{EM}=0$ and examining the resulting expressions, the appropriate value of $\bar{\mu}_i$ can be determined by

$$\bar{\mu}_2=\bar{\mu}_3=-\frac{\sin^3\bar{q}_3}{4\ \sin\ 2\eta\sin^5(\bar{q}_3/2)}(5\ \cos\ \eta-7\ \cos(\bar{q}_3-\eta)+3\ \cos(2\bar{q}_3-\eta)-\ \cos(\bar{q}_3+\eta))\bar{\mu}_1 \tag{42}$$

The resulting inter-craft electromagnetic forces are expressed as

$$\begin{cases}\bar{\mathbf{F}}_{12}^{EM}=\begin{bmatrix}-\frac{3\mu_0\bar{\mu}_1\bar{\mu}_2}{512\pi\bar{q}^4\sin^5(\bar{q}_3/2)}(7\ \sin(\bar{q}_3-\eta)-5\ \sin(2\bar{q}_3-\eta)-\ \sin(\eta+\bar{q}_3)+3\ \sin\ \eta)\\ -\frac{3\mu_0\bar{\mu}_1\bar{\mu}_2}{512\pi\bar{q}^4\sin^5(\bar{q}_3/2)}(5\ \cos(\bar{q}_3-\eta)-5\ \cos(2\bar{q}_3-\eta)-\ \cos(\eta+\bar{q}_3)+\ \cos\ \eta)\\ 0\end{bmatrix}\\ \bar{\mathbf{F}}_{23}^{EM}=\begin{bmatrix}0\\ \frac{3\mu_0\bar{\mu}_2\bar{\mu}_3(\sin^2\eta-2)}{64\pi\bar{q}^4\sin^4\bar{q}_3}\\ 0\end{bmatrix},\ \bar{\mathbf{F}}_{31}^{EM}=\begin{bmatrix}-\bar{F}_{12x}^{EM}\\ \bar{F}_{12y}^{EM}\\ 0\end{bmatrix}\end{cases} \tag{43}$$

In addition, considering $\bar{F}_{2y}^{EM}=\bar{F}_{23y}^{EM}-\bar{F}_{12y}^{EM}\approx 0^+$, the value of η can quickly be determined by combining Eqs. (42) and (43), and satisfies

$$\begin{aligned}&\sin\ \bar{q}_3\ \sin\ 2\eta(5\ \cos(\bar{q}_3-\eta)-5\ \cos(2\bar{q}_3-\eta)-\ \cos(\eta+\bar{q}_3)+\ \cos\ \eta)\\ &=2(\sin^2\eta-2)(5\ \cos\ \eta-7\ \cos(\bar{q}_3-\eta)+3\ \cos(2\bar{q}_3-\eta)-\ \cos(\bar{q}_3+\eta))\end{aligned} \tag{44}$$

As discussed above, Eqs. (42)–(44) represent the shape solutions for desired isosceles triangle static electromagnetic formation with given $\bar{q}$, $\bar{q}_3$ and $\bar{\mu}_1$. The relationship of η and $\bar{q}_3$ based on Eq. (44) is illustrated in Fig. 5. It is important to note that η is not $\bar{q}_3/2$ except for the trivial case where $\bar{q}_3\approx 109.05^\circ$ to make $\bar{\boldsymbol{\mu}}_2$, $\bar{\boldsymbol{\mu}}_3$ point to craft 1. The reason is some components of electromagnetic force should be used to counteract the influence of the gravity. In particular, when $\bar{q}_3=2\pi/3$, the triangular configuration is simplified to an equilateral triangle with three craft equal mass, and $\eta\approx 58.345^\circ$ is numerically solved. Accordingly, the ratio relation between $\bar{\mu}_i$ based on Eq. (42) is illustrated in Fig. 6.

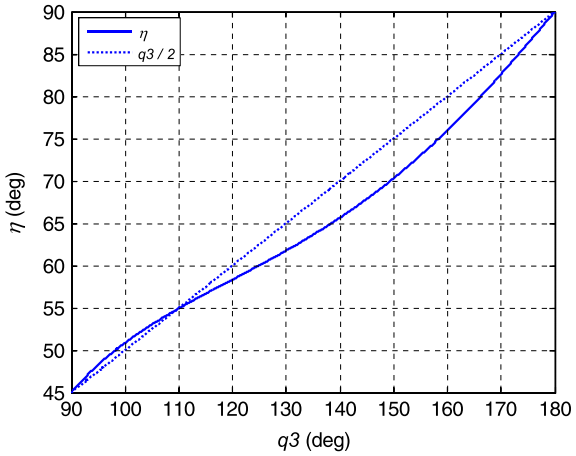

Fig. 5. Relation between η and $\bar{q}_3$.

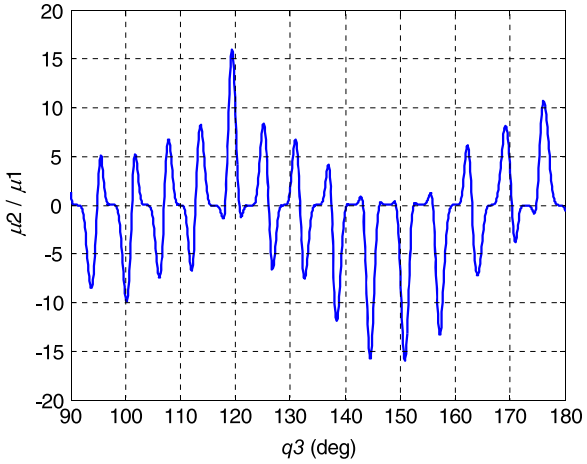

Fig. 6. Ratio between $\bar{\mu}_2$ and $\bar{\mu}_1$.

4. Shape solutions of spinning configurations

The invariant shape also yields spinning configurations about the collective center of mass. This section investigates whether such three-craft invariant shapes with real and constant magnetic moments are feasible for collinear and triangular configurations respectively. It is important to recognize that not all the derivation of $\bar{q}_i$ are zero at such equilibrium because of the existence of spin rate ξ.

4.1. Spinning collinear configuration

The three cases where the collinear configuration spins about each of three $\mathscr{H}$-frame axes are considered here respectively. Based on the dynamic model for the along-track configuration, the case of collinear configuration spinning about axis $\hat{x}_{CM}$ is studied first. As shown in Fig. 2(a), defining $\boldsymbol{\xi} = \xi \hat{\mathbf{x}}_{CM}$, if such relative equilibrium is maintained, we have $\bar{q}_3 = 0$, $\bar{q}_4 \neq 0$, $\dot{\bar{q}}_4 = \xi \neq 0$, thus $\bar{u}_3 = \Omega$, $\bar{u}_4 = \xi$. By examining the equilibrium conditions of relative attitude motion in Eq. (10), the magnetic torques should satisfy

$$\begin{cases} \bar{\tau}_{1x}^{EM} = I_1 \dot{\xi},\ \bar{\tau}_{1y}^{EM} = I_1 \Omega \xi c_4,\ \bar{\tau}_{1z}^{EM} = -I_1 \Omega \xi s_4 \\ \bar{\tau}_{2x}^{EM} = I_2 \dot{\xi},\ \bar{\tau}_{2y}^{EM} = I_2 \Omega \xi c_4,\ \bar{\tau}_{2z}^{EM} = -I_2 \Omega \xi s_4 \\ \bar{\tau}_{3x}^{EM} = I_3 \dot{\xi},\ \bar{\tau}_{3y}^{EM} = I_3 \Omega \xi c_4,\ \bar{\tau}_{3z}^{EM} = -I_3 \Omega \xi s_4 \end{cases} \tag{45}$$

Recalling angular momentum conservation for along-track configuration, $\bar{\tau}_{1y}^{EM} + \bar{\tau}_{2y}^{EM} + \bar{\tau}_{3y}^{EM} = 0$ must be met, which imply $\Omega = 0$ since $c_4 = 0$ is not always maintained. It is apparent that collinear configuration spinning about axis $\hat{x}_{CM}$ is not permissible with consideration of the gravity. Note that the value of $\dot{\xi}$ is not confined in above analysis, so this statement is

always true no matter whether $\dot{\xi}=0$. In addition, one can check that $\Omega=0$ is also required for invariant shape solution of collinear configuration spinning about axis $\hat{y}_{CM}$ under a similar consideration.

Next, considering the collinear configuration spinning about axis $\hat{z}_{CM}$, here let $\boldsymbol{\xi}=\xi\hat{\mathbf{z}}_{CM}$, so we have $\bar{q}_3\neq 0$, $\bar{q}_4=0$, $\dot{\bar{q}}_3=\xi\neq 0$, thus $\bar{u}_3=\Omega+\xi$. Following the same operation, $\dot{\xi}=0$ is required to maintain angular momentum conservation, then the equilibrium equations of motion are derived as

$$\begin{cases}\bar{q}_1(\Omega+\xi)^2-\mu\bar{q}_1/\bar{r}_1^3=\left(\bar{F}_{12y}^{EM}-\bar{F}_{31y}^{EM}\right)/m_1\\ \bar{q}_2(\Omega+\xi)^2-\mu\bar{q}_2/\bar{r}_2^3=-\left(\bar{F}_{23y}^{EM}-\bar{F}_{12y}^{EM}\right)/m_2\end{cases}\tag{46}$$

Actually, the equilibrium electromagnetic forces keep constant because of constant magnetic moments operated in an invariant shape, so the right sides of Eq. (46) keep constant as well. However, it is obvious that the left sides of Eq. (46) are time-varying since $\bar{r}_i$ change as crafts rotating in the orbital plane. The only solution to Eq. (46) is $\bar{r}_i\to\infty$ so as to give $\Omega=0$.

Base on the above analysis, we have a conclusive statement that the feasible invariant shape solutions for spinning three-craft collinear configurations only exist in the deep space without influence of the gravity. For the three-craft collinear configuration spinning in deep space, the only force acting on each craft is electromagnetic force, which offers a centripetal force to maintain rotation. Indeed, there are no differences for the collinear configuration spinning about which one of three axes in deep space. Let us study this problem based on Eq. (10). Then, the equilibrium equations of motion are simplified as

$$\begin{cases}\bar{F}_{12y}^{EM}-\bar{F}_{31y}^{EM}=m_1\bar{q}_1\xi^2>0\\ \bar{F}_{12y}^{EM}-\bar{F}_{23y}^{EM}=m_2\bar{q}_2\xi^2>0\end{cases}\tag{47}$$

which has a similar formulation with Eq. (32) except for reverse sign of the right side. Following the derivation presented in Section 3.1.2, we could identify that the possible shape solutions satisfying Eq. (47) have a similar formulation either, which will not be elaborated here. Note that the required electromagnetic forces for spinning equilibrium depend on spin rate $\boldsymbol{\xi}$, and the magnitudes of $\bar{\boldsymbol{\mu}}_i$ could be determined accordingly.

4.2. Spinning triangular configuration

Consider the triangular configuration spinning about axis $\hat{z}_B$ in the orbital plane or perpendicular to radial direction as Section 3.2. Similarly, the appropriate configuration constraints are examined by checking angular momentum conservation. Let $\boldsymbol{\xi}=\xi\hat{\mathbf{z}}_B$, for the triangular configuration spinning in the orbital plane, we have $\bar{q}_4=\bar{q}_6=0$, $\bar{q}_5\neq 0,\dot{\bar{q}}_5=\xi$, then $\bar{u}_6=\Omega+\xi$. So angular momentum conservation satisfies

$$(I_1+I_2+I_3)\dot{\xi}=m_1\bar{q}_1(\bar{f}_{1y}^{EM}-\bar{f}_{3y}^{EM})+m_2\bar{q}_2c_3(\bar{f}_{2y}^{EM}-\bar{f}_{3y}^{EM})+m_2\bar{q}_2s_3(\bar{f}_{2x}^{EM}-\bar{f}_{3x}^{EM})\tag{48}$$

which is true only when $\dot{\xi}=$ constant since the equilibrium electromagnetic forces and $\bar{q}_3$ maintain constant. Considering the fact that gravity for each craft in the orbital plane is time-varying periodically, it is impossible to offer a linear-varying centripetal force for each craft. Thus, the invariant shapes are not permissible for triangular configuration spinning in the orbital plane.

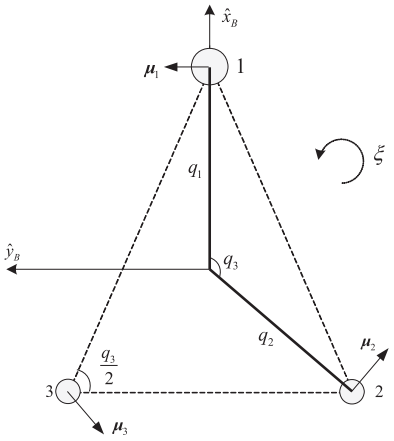

Fig. 7. Magnetic moments for three-craft triangular spinning configuration.

Next, if the spin axis $\hat{z}_B$ coincides with radial direction, we have $\bar{q}_4=\pi/2$, $\bar{q}_6=0$, $\bar{q}_5\neq 0$, $\dot{\bar{q}}_5\neq\xi$ at equilibrium, then $\bar{u}_4=-\Omega c_5$, $\bar{u}_5=\Omega s_5$, $\bar{u}_6=\xi$. Thus, $\dot{\xi}=0$ is required for a similar derivation, and angular momentum conservation satisfies

$$\begin{cases}\mu r_{cm}(1/\bar{r}_1^3-1/\bar{r}_3^3)=m_2\bar{q}_2\Omega\xi(c_3c_5+s_3s_5)/m_3+(m_1+m_3)\bar{q}_1\Omega\xi c_5/m_3\\ \mu r_{cm}(1/\bar{r}_2^3-1/\bar{r}_3^3)=(m_2+m_3)\bar{q}_2\Omega\xi(c_3c_5+s_3s_5)/m_3+m_1\bar{q}_1\Omega\xi c_5/m_3\end{cases} \tag{49}$$

Since $\bar{r}_i$ are constant for such configuration, $\Omega=0$ is the only solution to Eq. (49) with $\bar{r}_1=\bar{r}_2=\bar{r}_3$ being true accordingly, so that the formation geometry is an isosceles triangle with $\bar{q}_1=\bar{q}_2$, $m_2=m_3$ and $c_3=-m_1/2m_2$ following the analysis in Section 3.2. This means that there are no feasible invariant shape solutions except for the case where the three-craft triangular configuration spins without the influence of gravity.

Therefore, if such isosceles triangle configuration spins in deep space, the electromagnetic forces acting on each craft offer centripetal forces to maintain rotation. Here we only identify a particular solution of magnetic moments with $\bar{\mu}_{iz}=0$ for simplicity. Thus, the required accelerations of electromagnetic force are derived as

$$\begin{cases}\bar{f}_{1x}^{EM}=-\bar{q}\xi^2\\ \bar{f}_{1y}^{EM}=0\end{cases},\quad\begin{cases}\bar{f}_{2x}^{EM}=-\bar{q}c_3\xi^2\\ \bar{f}_{2y}^{EM}=\bar{q}s_3\xi^2\end{cases},\quad\begin{cases}\bar{f}_{3x}^{EM}=\bar{f}_{2x}^{EM}\\ \bar{f}_{3y}^{EM}=-\bar{f}_{2y}^{EM}\end{cases} \tag{50}$$

In this manner, the electromagnetic forces acting on all three crafts are pointing to the center of mass, so the magnetic moments should be arranged end to end in a circle, while the unit vector of $\bar{\boldsymbol{\mu}}_i$ is perpendicular to $\boldsymbol{\rho}_i$. As shown in Fig. 7, assume the magnetic moments for each craft as

$$\bar{\boldsymbol{\mu}}_1=\begin{bmatrix}0 & \bar{\mu}_1 & 0\end{bmatrix}^{\mathrm{T}},\ \bar{\boldsymbol{\mu}}_2=\begin{bmatrix}\bar{\mu}_2\sin\bar{q}_3 & \bar{\mu}_2\cos\bar{q}_3 & 0\end{bmatrix}^{\mathrm{T}},\ \bar{\boldsymbol{\mu}}_3=\begin{bmatrix}-\bar{\mu}_3\sin\bar{q}_3 & \bar{\mu}_3\cos\bar{q}_3 & 0\end{bmatrix}^{\mathrm{T}} \tag{51}$$

By substituting Eq. (51) into $\bar{\boldsymbol{\tau}}_i^{EM}=0$ and examining the resulting expressions, the appropriate value of $\bar{\mu}_i$ can be determined by

$$\bar{\mu}_2=\bar{\mu}_3=-\sin^3\bar{q}_3/(2\cos\bar{q}_3\sin^3(\bar{q}_3/2))\bar{\mu}_1 \tag{52}$$

The resulting inter-craft electromagnetic forces are expressed as

$$\begin{cases}\bar{\mathbf{F}}_{12}^{EM}=\begin{bmatrix}\frac{3\mu_0\bar{\mu}_1\bar{\mu}_2}{512\pi\bar{q}^4\sin^5(\bar{q}_3/2)}(\cos 2\bar{q}_3+2\cos\bar{q}_3-5)\\ -\frac{3\mu_0\bar{\mu}_1\bar{\mu}_2}{128\pi\bar{q}^4\sin^5(\bar{q}_3/2)}\sin\bar{q}_3(1+\cos^2(\bar{q}_3/2))\\ 0\end{bmatrix}\\ \bar{\mathbf{F}}_{23}^{EM}=\begin{bmatrix}0\\ -\frac{3\mu_0\bar{\mu}_2\bar{\mu}_3(\sin^2\bar{q}_3-2)}{64\pi\bar{q}^4\sin^4\bar{q}_3}\\ 0\end{bmatrix},\ \bar{\mathbf{F}}_{31}^{EM}=\begin{bmatrix}-\bar{F}_{12x}^{EM}\\ \bar{F}_{12y}^{EM}\\ 0\end{bmatrix}\end{cases} \tag{53}$$

In particular, when $\bar{q}_3=2\pi/3$, the triangular configuration is simplified to an equilateral triangle with three crafts share equal mass, thus we have $\bar{\mu}_1=\bar{\mu}_2=\bar{\mu}_3$.

So far, we have identified the feasible static or spinning invariant shape solutions for collinear and triangular configuration respectively. However, whether these equilibrium shapes are stable or not remains unknown, which would be discussed in the following section.

5. Linear stability analysis

To determine stability properties of an invariant shape, the linearization for equations of motion is developed about the corresponding relative equilibrium accordingly. Considering the dynamics described by generalized coordinates and generalized speeds, the state variables are chosen as $\mathbf{x}=[\mathbf{q}^{\mathrm{T}}\ \ \mathbf{u}^{\mathrm{T}}]^{\mathrm{T}}$, and the control variables are $\mathbf{u}_c=[\boldsymbol{\mu}_1^{\mathrm{T}}\ \ \boldsymbol{\mu}_2^{\mathrm{T}}\ \ \boldsymbol{\mu}_3^{\mathrm{T}}]^{\mathrm{T}}$. Assuming that all motions are small perturbations relative to the equilibrium point, we define $\mathbf{q}=\bar{\mathbf{q}}+\delta\mathbf{q}$, $\mathbf{u}=\bar{\mathbf{u}}+\delta\mathbf{u}$, $\mathbf{u}_c=\bar{\mathbf{u}}_c+\delta\mathbf{u}_c$. Based on the first order Taylor series approximation, the linearized dynamics can be

Table 1
Shape parameters corresponding to different static configurations.

	Configurations	δ	σ	χ
(a)	Along-track collinear configuration	1.0	1.0	1.0
(b)		0.5	4.750	1.5
(c)	Orbit normal collinear configuration	0.5	4.786	1.5
(d)	Equilateral triangle configuration	1.0	1.0	1.0

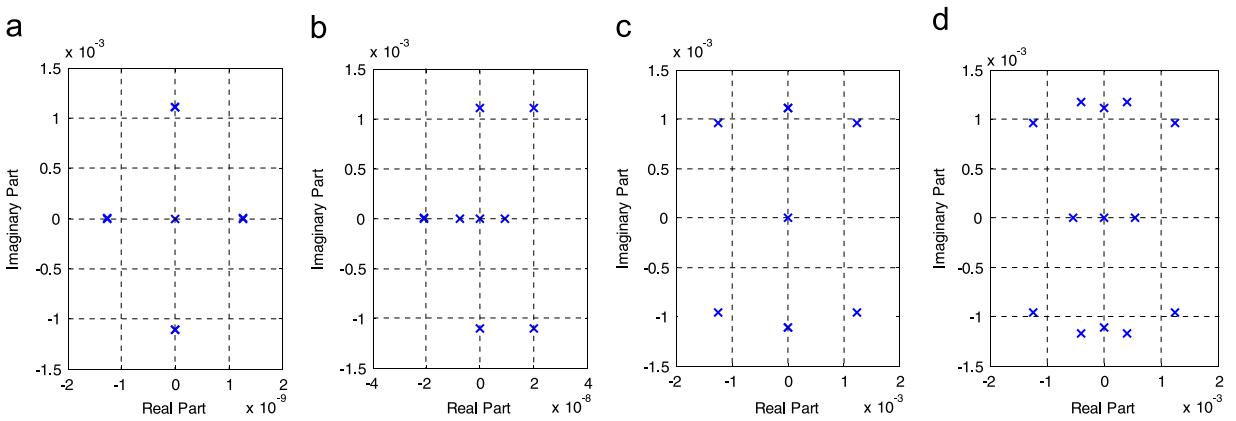

Fig. 8. Open-loop eigenvalues for different configurations in Table 1.

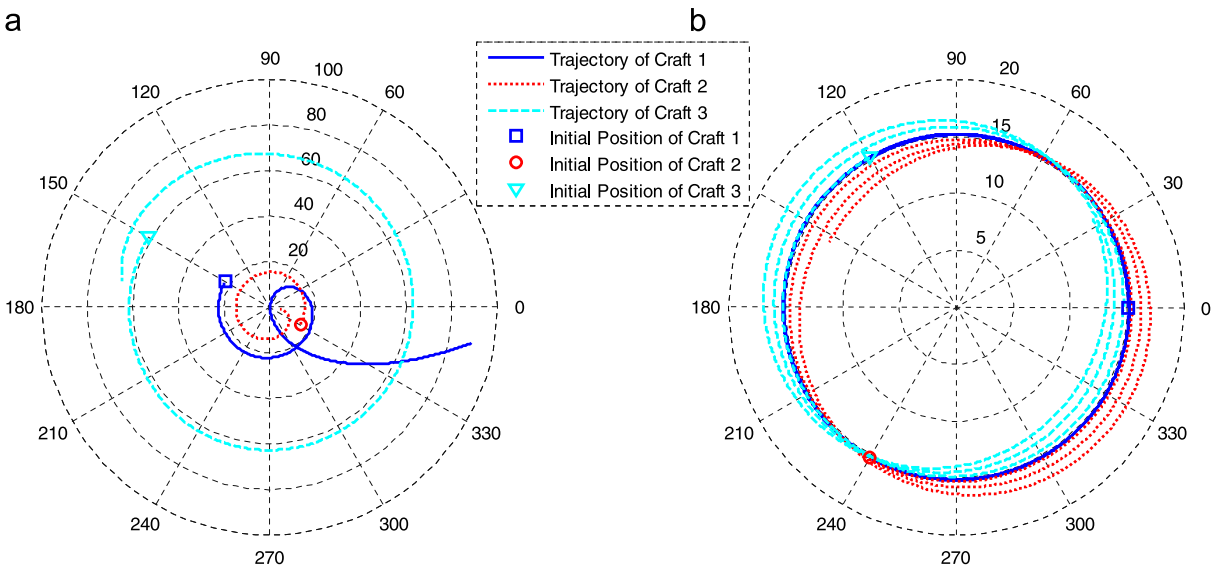

Fig. 9. Perturbed trajectory for (a) collinear and (b) equilateral triangle spinning configuration.

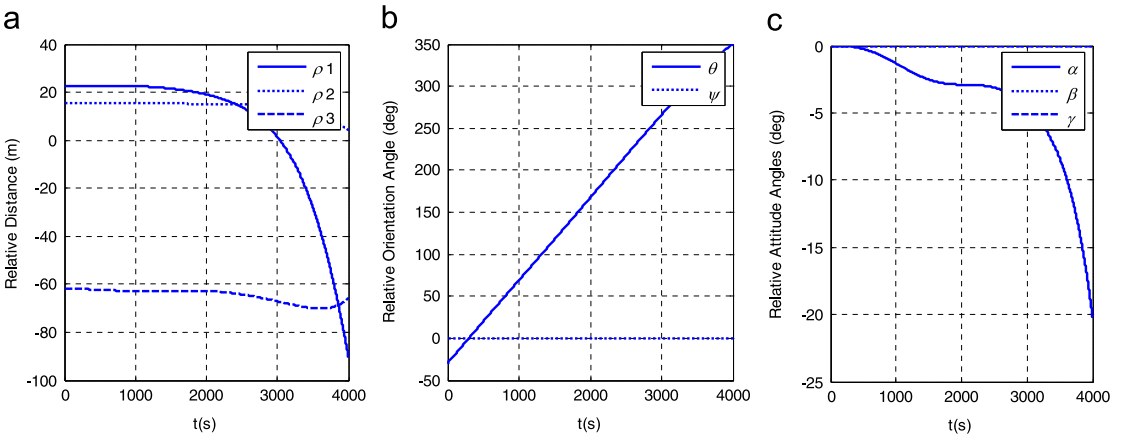

Fig. 10. State curves for spinning collinear configuration.

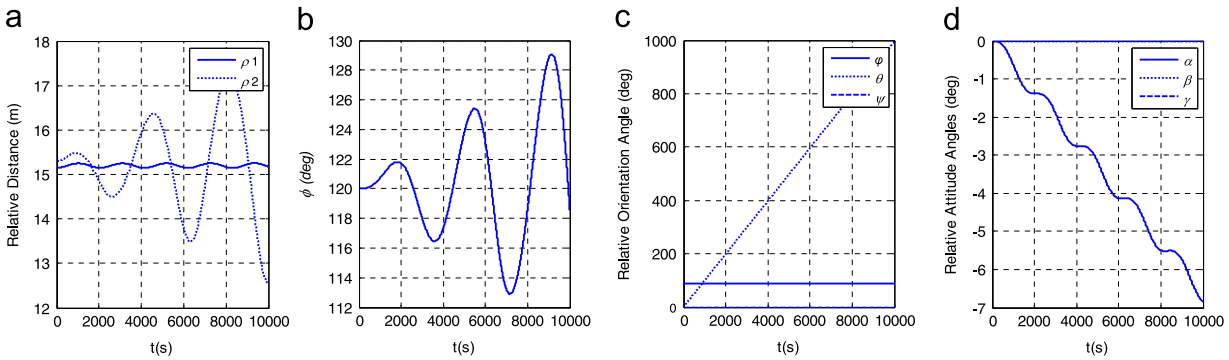

Fig. 11. State curves for spinning equilateral triangle configuration.

expressed as

$$\delta\dot{\mathbf{x}} = \mathbf{A}(\bar{\mathbf{q}},\ \bar{\mathbf{u}},\ \bar{\mathbf{u}}_c)\delta\mathbf{x} + \mathbf{B}(\bar{\mathbf{q}},\ \bar{\mathbf{u}},\ \bar{\mathbf{u}}_c)\delta\mathbf{u}_c = \begin{bmatrix} \partial\dot{\mathbf{q}}/\partial\mathbf{q}^{\mathrm{T}} & \partial\dot{\mathbf{q}}/\partial\mathbf{u}^{\mathrm{T}} \\ \partial\dot{\mathbf{u}}/\partial\mathbf{q}^{\mathrm{T}} & \partial\dot{\mathbf{u}}/\partial\mathbf{u}^{\mathrm{T}} \end{bmatrix}_{\bar{\mathbf{q}},\bar{\mathbf{u}},\bar{\mathbf{u}}_c} \begin{bmatrix} \delta\mathbf{q} \\ \delta\mathbf{u} \end{bmatrix} + \frac{\partial\dot{\mathbf{x}}}{\partial\mathbf{u}_c^{\mathrm{T}}}\Big|_{\bar{\mathbf{q}},\bar{\mathbf{u}},\bar{\mathbf{u}}_c} \delta\mathbf{u}_c \tag{54}$$

where Jacobin matrix **A**, **B** are evaluated at the equilibrium point $\bar{\mathbf{x}}$, $\bar{\mathbf{u}}_c$, and the eigenvalues of matrix **A** can be computed to assess the stability properties of the above shapes. Since the formulations of the elements in **A**, **B** are too complicated to be briefly recognized, we will numerically discuss the eigenvalues, as well as the linear stability for different families of invariant shapes.

As an example, for the invariant shapes of static configuration, consider a three-craft formation where the formation center of mass travels in a circular orbit of 500 km. Choosing the shape parameters as shown in Table 1 for illustration. Let $\bar{q}_2 = 15\ m$, $m_3 = 150$ kg, $I_3 = 20$ kg m^2, the resulting numerical eigenvalues for different configurations are shown in Fig. 8. It is obvious that all these cases have eigenvalues with real parts to make the static configuration unstable.

For the invariant shapes of spinning configuration, consider a three-craft formation operating in deep space. Choose the same shape parameters as shown in Tables 1(c) and 1(d) for collinear and triangular configuration respectively. Assuming the spin rate is $\xi = 2\pi$ rad/h, the corresponding invariant shapes are numerically ensured without perturbation. Here, an initial perturbation of $\delta q_1 = 0.01$ m and $\delta q_2 = 0.02$ m are applied and the full nonlinear equations are integrated to examine the stability. The resulting perturbed trajectories and state curves under constant electromagnetic forces are shown as Fig. 9–11, where the relative attitude curves are only presented for one of three crafts to illustrate. It is apparent that the spinning configurations are all unstable, especially the collinear configuration diverges from the equilibrium point much faster. This is because the real part of unstable eigenvalues of the collinear configuration 0.001745 is much bigger than that of triangular configuration 2.5×10^{-11}.

Again, we numerically assess the controllability of such invariant shapes. From the linear control theory, we know that the system is only controllable if

$$\mathrm{rank}(\mathbf{C}) = \mathrm{rank}\left([\mathbf{B} \quad \mathbf{AB} \quad \mathbf{A}^2\mathbf{B} \quad \ldots \quad \mathbf{A}^{n-1}\mathbf{B}]\right) = n \tag{55}$$

where **C** is the controllability matrix. Calculating **A**, **B** by the parameters in Table 1 and substituting in Eq. (55), we can check that the ranks of collinear and triangular configuration are 26 and 30 respectively, which both satisfying Eq. (55). Hence the full nonlinear systems are controllable within small deviation around the equilibrium.

Actually, the open-loop eigenvalues and controllability for other invariant shapes can also be determined following same procedures. We have examined that most of these shapes are unstable and controllable so far, but no guarantee whether a stable or marginally stable solution do exist since there are an infinite number of solutions for any desired invariant shape. Moreover, in order to maintain these shapes, an active magnetic moment control needs to be performed. Resolution of these problems would be left for future work.

6. Conclusion

Concentrating on the invariant shape for close formation flying with inter-craft electromagnetic force, this paper mainly analyzes the invariant shapes of relative equilibrium for three-craft electromagnetic formation, and studies the families of invariant shape solutions and their linear stability. Both collinear and general triangular configurations are considered under the full nonlinear coupled dynamic models. By analyzing the 6-DOF relative equilibrium problem, the magnetic moments and geometry conditions to guarantee feasibility of the invariant shape, and the corresponding families of invariant shape solutions with real and constant magnetic moments are identified for static and spinning configurations respectively. Especially, some particular interesting shapes are chosen to illustrate the results and convenient control. Furthermore, numerical simulations are carried out to analyze the linear stability, which show that most invariant shapes

for the three-craft electromagnetic formation are unstable and controllable, and active control is required to maintain these configurations.

Acknowledgments

This work is supported in part by a grant from the National Natural Science Foundation of China (11172322). The author would like to acknowledge my colleague Ms. Wang-qiong Peng for her revising suggestions in the paper's English writing.

References

[1] P.R. Lawson, J.A. Dooley. Technology plan for the terrestrial planet finder interferometer, Technical Report, JPL Publication 05-5, NASA Jet Propulsion Lab, June 2005.
[2] L.B. King, G.G. Parker, S. Deshmukh, J. Chong, Spacecraft Formation-Flying Using Inter-Vehicle Coulomb Forces, Michigan Technological University, Massachusetts, 2002.
[3] L.M. Elias, S.A. Schweighart, D.W. Kwon, D. LoBosco. Electromagnetic formation flight final report, Technical Report, Massachusetts Institute of Technology, 2004.
[4] D.W. Kwon, Propellantless formation flight applications using electromagnetic satellite formations, Acta Astronaut. 67 (2010) 1189–1201.
[5] H. Schaub, C.D. Hall, J. Berryman, Necessary conditions for circularly-restricted static coulomb formations, J. Astronaut. Sci. 54 (3) (2006) 525–541.
[6] J. Berryman, H. Schaub, Analytical charge analysis for two- and three-craft coulomb formations, J Guidance Control Dyn. 30 (6) (2007) 1701–1710.
[7] A. Natarajan., A Study of Dynamics and Stability of Two-Craft Coulomb Tether Formations, Virginia Polytechnic Institute and State University, Virginia, 2007.
[8] R. Inampudi, H. Schaub. Orbit radial dynamic analysis of two-craft coulomb formation at libration points, in: Proceedings of the AIAA/AAS Astrodynamics Specialist Conference, Toronto, Canada, 2–5 August 2010.
[9] H. Schaub, I.I. Hussein, Stability and reconfiguration analysis of a circularly spinning two-craft Coulomb tether, IEEE Trans. Aerosp. Electron. Syst. 46 (4) (2010) 1675–1685.
[10] I.I. Hussein, H. Schaub, Invariant shape solutions of the spinning three craft Coulomb tether problem, Celestial Mech. Dynamical Astron. 96 (2006) 137–157.
[11] I.I. Hussein, H. Schaub, Stability and control of relative equilibria for the three-spacecraft coulomb tether problem, Acta Astronaut. 65 (2009) 738–754.
[12] S. Wang, H. Schaub, Nonlinear charge control for a collinear fixed shape three-craft equilibrium, in: Proceedings of the AIAA Guidance, Navigation and Control Conference, Toronto, Canada, 2–5 August 2010.
[13] E.A. Hogan, H. Schaub, Collinear invariant shapes for three-spacecraft Coulomb formations, Acta Astronaut. 72 (2012) 78–89.
[14] E.A. Hogan, H. Schaub, Linear stability and shape analysis of spinning three-craft Coulomb formations, Celestial Mech. Dynamical Astron. 112 (2012) 131–148.
[15] L.M. Elias, D.W. Kwon, R.J. Sedwick, D.W. Miller, Electromagnetic formation flight dynamics including reaction wheel gyroscopic stiffening effects, J Guidance Control Dyn. 30 (2) (2007) 499–511.
[16] S.A. Schweighart, Electromagnetic Formation Flight Dipole Solution Planning, Massachusetts Institute of Technology, USA, 2005.
[17] U. Ahsun, D.W. Miller, J.L. Ramirez, Control of electromagnetic satellite formations in near-earth orbits, J Guidance Control Dyn. 33 (6) (2010) 1883–1891.
[18] D.W. Kwon, R.J. Sedwick, S. Lee, J.L. Ramirez-Riberos, Electromagnetic formation flight testbed using superconducting coils, J. Spacecr. Rockets 48 (1) (2011) 124–133.
[19] D.W. Miller, R.J. Sedwick, E.M. Kong, S.A. Schweighart, Electromagnetic formation flight for sparse aperture telescopes, in: Proceedings of the 2002 IEEE Aerospace Conference, Big Sky, Montana, 9–16 March 2002.
[20] E.M. Kong, D.W. Kwon, S.A. Schweighart, L.M. Elias, Electromagnetic formation flight for multisatellite arrays, J. Spacecr. Rockets 41 (4) (2004) 659–666.
[21] I.I. Hussein, A.M. Bloch, Stability and control of relative equilibria of three-spacecraft magnetically tethered systems, in: Proceedings of the AIAA/AAS Astrodynamics Specialist Conference and Exhibit, Honolulu, Hawaii, 18–21 August 2008.